

Review

Recent Progress in Metal Borohydrides for Hydrogen Storage

Hai-Wen Li ^{1,*}, Yigang Yan ¹, Shin-ichi Orimo ¹, Andreas Züttel ² and Craig M. Jensen ³

¹ Institute for Materials Research (IMR), Tohoku University, Sendai 980-8577, Japan;
E-Mails: yg-yan@imr.tohoku.ac.jp (Y.Y.); orimo@imr.tohoku.ac.jp (S.O.)

² Department of the Environment, Energy and Mobility (EMPA), Abt. 138 “Hydrogen & Energy”,
Überlandstrasse 129, 8600 Dübendorf, Switzerland; E-Mail: Andreas.Zuetzel@empa.ch

³ Department of Chemistry, University of Hawaii, Honolulu, HI 96822, USA;
E-Mail: jensen@hawaii.edu

* Author to whom correspondence should be addressed; E-Mail: lihw@imr.tohoku.ac.jp;
Tel.: +81-22-215-2093; Fax: +81-22-215-2091.

Received: 23 November 2010; in revised form: 22 December 2010 / Accepted: 17 January 2011 /
Published: 24 January 2011

Abstract: The prerequisite for widespread use of hydrogen as an energy carrier is the development of new materials that can safely store it at high gravimetric and volumetric densities. Metal borohydrides $M(\text{BH}_4)_n$ (n is the valence of metal M), in particular, have high hydrogen density, and are therefore regarded as one such potential hydrogen storage material. For fuel cell vehicles, the goal for on-board storage systems is to achieve reversible store at high density but moderate temperature and hydrogen pressure. To this end, a large amount of effort has been devoted to improvements in their thermodynamic and kinetic aspects. This review provides an overview of recent research activity on various $M(\text{BH}_4)_n$, with a focus on the fundamental dehydrogenation and rehydrogenation properties and on providing guidance for material design in terms of tailoring thermodynamics and promoting kinetics for hydrogen storage.

Keywords: hydrogen; hydride; borohydride; hydrogen storage

1. Introduction

Development of advanced hydrogen storage materials for onboard hydrogen storage systems is regarded as a key prerequisite for widespread adoption of fuel cell vehicles. For commercial vehicle

applications, hydrogen storage materials must possess all the following capabilities: high gravimetric hydrogen density, adequate hydrogenation-dehydrogenation temperature/rate, cycling stability, and low cost [1].

Metal borohydrides $M(BH_4)_n$ (n indicates the valence of M) have high gravimetric hydrogen densities and thus have attracted great interest for use in hydrogen storage [2]. The gravimetric hydrogen densities and physical properties of various $M(BH_4)_n$ [3] are shown in Figure 1 and Table 1, respectively.

Figure 1. Elements M formed $M(BH_4)_n$, their gravimetric hydrogen densities in the unit of mass%. Asterisks indicate compounds stabilized at room temperature by coordination with ligands. Brackets indicate compounds reported to be unstable at room temperature but may be isolated at low temperature [3]. Reproduced with permission from reference 3.

| | | | | | | | | | | | | | | | | | | | |
|------|------|------|---------------------------|-------------------------|-----|------|------|------|------|-------|------|------|------|-----|-----|--|--|----|----|
| 1 | 2 | | | | | | | | | | | | | | | | | | |
| Li | Be | | | | | | | | | | | | | | | | | | |
| 18.5 | 20.8 | | | | | | | | | | | | | | | | | | |
| Na | Mg | | | | | | | | | | | | | | | | | 13 | 14 |
| 10.7 | 14.9 | 3 | 4 | 5 | 6 | 7 | 8 | 9 | 10 | 11 | 12 | [Al] | | | | | | | |
| | | | | | | | | | | | | 16.9 | | | | | | | |
| K | Ca | Sc | Ti | V | Cr | [Mn] | [Fe] | [Co] | [Ni] | [Cu]* | Zn | [Ga] | Ge | | | | | | |
| 7.5 | 11.6 | 13.5 | III 13.1 IV 15.0 | 12.7 | 9.9 | 9.5 | 9.4 | 9.1 | 9.1 | 5.1 | 4.4 | 10.6 | 12.2 | | | | | | |
| Rb | Sr | Y | Zr | Nb | | | | | | [Ag]* | [Cd] | [In] | [Sn] | | | | | | |
| 4.0 | 6.9 | 9.1 | 10.7 | 8.8 | | | | | | 3.3 | 2.9 | 7.6 | 9.1 | | | | | | |
| Cs | Ba | Ln | Hf | | | | | | | [Au] | Hg | Tl | | | | | | | |
| 2.7 | 4.8 | | 6.8 | | | | | | | 1.9 | 1.8 | 4.9 | | | | | | | |
| | | Ac | | | | | | | | | | | | | | | | | |
| Ln | La | Ce | | Nd | | Sm | Eu | Gd | Tb | Dy | Ho | Er | Tm | Yb | Lu | | | | |
| | 6.6 | 6.6 | | 6.4 | | 6.2 | 6.2 | 6.0 | 5.9 | 5.8 | 5.8 | 5.7 | 5.7 | 5.6 | 5.5 | | | | |
| Ac | | Th | Pa | U | Np | Pu | | | | | | | | | | | | | |
| | | 5.5 | 5.6 | III 4.3 IV 5.4 | 5.4 | 5.4 | | | | | | | | | | | | | |

Table 1. Density of $M(BH_4)_n$ and hydrogen density in $M(BH_4)_n$ [3]. Reproduced with permission from reference 3.

| $M(BH_4)_n$ | CAS No. | Density (g/mol) | Density (g/cm ³) | Hydrogen Density (mass%) | Hydrogen Density (kg/m ³) |
|-----------------------------------|------------|-----------------|------------------------------|--------------------------|---------------------------------------|
| LiBH ₄ | 16949-15-8 | 21.78 | 0.66 | 18.5 | 122.1 |
| NaBH ₄ | 16940-66-2 | 37.83 | 1.07 | 10.7 | 114.5 |
| KBH ₄ | 13762-51-1 | 53.94 | 1.17 | 7.5 | 87.8 |
| RbBH ₄ | 20346-99-0 | 100.31 | 1.92 | 4.0 | 76.8 |
| CsBH ₄ | - | 147.75 | 2.42 | 2.7 | 65.3 |
| Be(BH ₄) ₂ | 17440-85-6 | 38.70 | 0.702 | 20.8 | 146.0 |
| Mg(BH ₄) ₂ | 16903-37-0 | 53.99 | 0.989 | 14.9 | 147.4 |
| Ca(BH ₄) ₂ | 17068-95-0 | 69.76 | (1.07) | 11.6 | (124.1) |
| Mn(BH ₄) ₂ | - | 84.62 | (1.24) | 9.5 | (117.8) |
| Al(BH ₄) ₃ | 16962-07-5 | 71.51 | 0.79 | 16.9 | 133.5 |
| Zr(BH ₄) ₄ | 12370-59-1 | 150.6 | 1.179 | 10.7 | 126.2 |
| Hf(BH ₄) ₄ | 53608-70-1 | 237.6 | 1.65 | 6.8 | 112.2 |

Densities in brackets shows the value calculated from the crystal structure.

First-principles calculations of the electronic structures of $M(\text{BH}_4)_n$ show that they are nonmetallic and have relatively large energy gaps of 1.8–6.8 eV. A boron atom forms covalent bonds with four surrounding H atoms to form $[\text{BH}_4]^-$ anions, the charge of which is compensated by metal cations M^{n+} . The electronic structures indicate that charge transfer from the metal cations M^{n+} to the $[\text{BH}_4]^-$ anions is a key feature determining the thermodynamic stability of $M(\text{BH}_4)_n$ [4–8].

Some $M(\text{BH}_4)_n$ have been used as “one-way” hydrogen sources that release the hydrogen on contact with water (via hydrolysis) [9–11]. Because the hydrolysis reaction is highly irreversible, such materials are certainly not candidates for reversible hydrogen storage. In this review, we focus on the recent progress in the dehydrogenation and rehydrogenation reactions of $M(\text{BH}_4)_n$ at controlled temperature and hydrogen pressure. Some several excellent reviews on $M(\text{BH}_4)_n$ are also available [2,12–18].

2. Fundamentals of Hydrogen Storage Properties

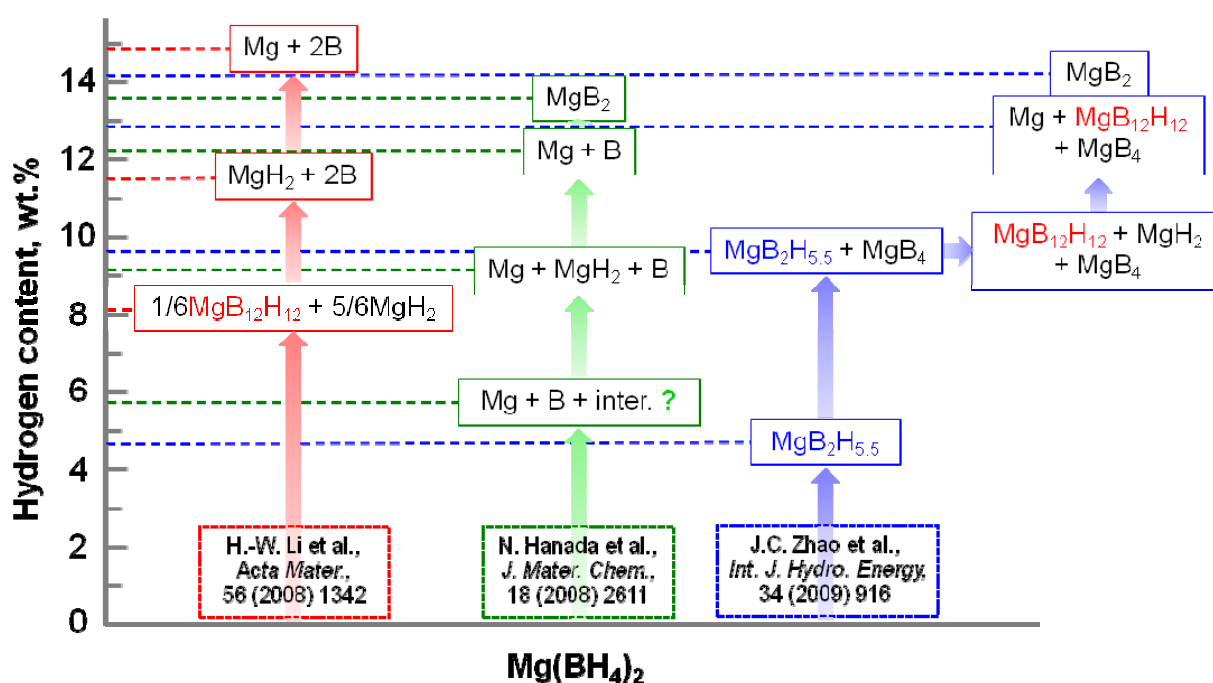
The study of $M(\text{BH}_4)_n$ as a candidate hydrogen storage material started with LiBH_4 [19]. It releases 13.8 mass% of hydrogen by decomposition into LiH and B [19–25]. The dehydrogenation process at a low heating rate (0.5 K/min) exhibits three distinct desorption peaks, which indicates that it involves several intermediate steps [25]. This was recently explained by the formation of $\text{Li}_2\text{B}_{12}\text{H}_{12}$ as an intermediate compound, evidenced by Raman and solid-state CP/MAS NMR analyses, as well as theoretical prediction [26–29]. $\text{Li}_2\text{B}_{12}\text{H}_{12}$ has a cubic crystal structure with $Pa\bar{3}$ symmetry [30]. A mechanistic explanation of the formation of $\text{Li}_2\text{B}_{12}\text{H}_{12}$ indicates that the diborane or higher borane species formed during the decomposition of LiBH_4 would react with the remaining LiBH_4 to afford $\text{Li}_2\text{B}_{12}\text{H}_{12}$ and possibly even $\text{Li}_2\text{B}_{10}\text{H}_{10}$ [31]. To understand the mechanism of dehydrogenation better, intensive investigations on the dynamics have been performed, including on the rotational and vibration motions of BH_4 tetrahedra; the atomic motions of H, Li, and B; H–D exchange in BH_4 units, *etc.* [32–50]. The enthalpy ΔH and entropy ΔS of dehydrogenation were found to be $74 \text{ kJ mol}^{-1} \text{ H}_2$ and $115 \text{ J K}^{-1} \text{ mol}^{-1} \text{ H}_2$, respectively, based on the pressure-concentration-temperature (PCT) isotherm measurement [51].

Dehydrogenation of LiBH_4 is reversible, because the end products lithium hydride (LiH) and boron absorb hydrogen at 873 K in a hydrogen pressure of 35 MPa for 12 h [23] or at 1000 K under a hydrogen pressure of 15 MPa for over 10 h [25] to form LiBH_4 . The high rehydrogenation temperature of above 873 K might be due to the sluggish kinetics of rehydrogenation, which requires recombination of the dehydrogenated LiH and B , that is, breaking of the rigid boron lattice, and the subsequent diffusion of Li and B atoms toward each other would be mainly responsible for the sluggish kinetics. The sluggish kinetics can be enhanced by preparing a homogenous dispersion of Li and B atoms on an atomic level. For example, forming a binary LiB_x compound (e.g., Li_7B_6 , LiB_3 , and LiB , *etc.*) has been proved to significantly improve the reaction kinetics of LiBH_4 formation over that of the Li/B mixture [51–53]. In addition, the formation of LiBH_4 might be related to diborane B_2H_6 [53–55].

$\text{Mg}(\text{BH}_4)_2$ releases approximately 14.9 mass% of hydrogen when heated up to 870 K [56–66]. The dehydrogenation process is found to also proceed through multiple steps together with the formation of intermediate compounds [62,63,65], as summarized in Figure 2. Thus far, one of the intermediate

compounds has been theoretically predicted and experimentally confirmed as being $\text{MgB}_{12}\text{H}_{12}$ [28,29,62,65–70] similar to that in the case of LiBH_4 [26]. The lowest energy configuration of $\text{MgB}_{12}\text{H}_{12}$ was predicted as being monoclinic in the space group $C2/m$ (No. 12) [29]. Anhydrous $\text{MgB}_{12}\text{H}_{12}$ cannot be obtained from simple thermal decomposition of $\text{Mg}(\text{H}_2\text{O})_6\text{B}_{12}\text{H}_{12}\cdot 6\text{H}_2\text{O}$ [71]. The apparent enthalpy and entropy for the conversion of $\text{Mg}(\text{BH}_4)_2$ to MgH_2 were estimated from PCT measurement to be $39 \text{ kJ mol}^{-1} \text{ H}_2$ and $91 \text{ J K}^{-1} \text{ mol}^{-1} \text{ H}_2$ [56], respectively. In a later work, different values were reported: $\Delta H = 57 \text{ kJ mol}^{-1} \text{ H}_2$ and $\Delta S = 128 \text{ J K}^{-1} \text{ mol}^{-1} \text{ H}_2$ [62]. These differences might originate from differences in the measurement conditions. For example, a shorter equivalent judgment time will lead to a higher plateau due to the sluggish kinetics.

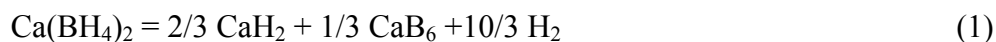
Figure 2. The dehydrogenation processes of $\text{Mg}(\text{BH}_4)_2$ based on the respective reports. Question mark indicates the possibility of the formation of an intermediate compound during the dehydrogenation.



Rehydrogenation of $\text{Mg}(\text{BH}_4)_2$ occurs at 543 K in a hydrogen pressure of 40 MPa for 48 h. Approximately 6.1 mass% of hydrogen is rehydrogenated through the formation of $\text{MgB}_{12}\text{H}_{12}$ [62,66]. The formation of $\text{MgB}_{12}\text{H}_{12}$, rather than $\text{Mg}(\text{BH}_4)_2$, after rehydrogenation may be explained from the viewpoint of the crystal (cluster) structure. The formation of $\text{Mg}(\text{BH}_4)_2$ is more thermodynamically favorable than that of $\text{MgB}_{12}\text{H}_{12}$ from the dehydrogenated products (MgH_2 and boron) at 573 K. However, for the formation of $\text{Mg}(\text{BH}_4)_2$, the B–B bonds in the icosahedral cluster of B should be broken and the B atoms should spatially migrate to form $[\text{BH}_4]^-$. The barrier against breaking of the B–B bonds and migration of the B atoms is probably too high to overcome under the present rehydrogenation conditions [66]. However, it is almost the same boron icosahedral clusters in between B and $\text{MgB}_{12}\text{H}_{12}$ that facilitate the formation of $[\text{B}_{12}\text{H}_{12}]^{2-}$. In other words, the formation of $\text{Mg}(\text{BH}_4)_2$ requires higher temperature and pressure to overcome the aforementioned barriers. This was proven in a recent study: partial formation of $\text{Mg}(\text{BH}_4)_2$ was confirmed in rehydrogenation experiments carried out at 663 K in a hydrogen pressure of 90 MPa for 3 days [72]. In addition, $\text{Mg}(\text{BH}_4)_2$ can be prepared

by hydrogenation of MgB_2 at 673 K under a hydrogen pressure of 90 MPa for a few days [73]. This hydrogenation reaction can be greatly promoted by using nanostructures with grain boundary defects introduced by mechanical milling [73–75]. Recently, $\text{Mg}(\text{BH}_4)_2$ was found to be formed by hydrogenation of $\text{Mg}(\text{B}_3\text{H}_8)_2$ at 523 K under a hydrogen pressure of 12 MPa [76].

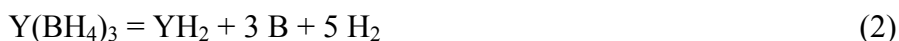
$\text{Ca}(\text{BH}_4)_2$ was theoretically predicted to release 9.6 mass% of hydrogen according to the following reaction [77]:



Experimentally, approximately 9.0 mass% of hydrogen was released when $\text{Ca}(\text{BH}_4)_2$ was heated to 800 K [78–80]. This value shows good agreement with that predicted by Equation 1. The presence of two endothermic peaks corresponding to dehydrogenation suggests the formation of intermediate compounds, which is confirmed by the powder X-ray diffraction (XRD) analyses of the dehydrogenated products that were heated to approximately 663 K [78] and after the plateau in the PCT profile measured at 593 K [79]. The intermediate compound is suggested to be a CaB_2H_x compound having a HgCl_2 -type structure with $Pnma$ symmetry according to the high-resolution synchrotron radiation powder XRD measurement [81]. By contrast, the proposed CaB_2H_x was predicted to be both structurally unstable and too high in energy to be a dehydrogenation intermediate based on the plane wave density functional theory calculations [82]. The formation of $\text{CaB}_{12}\text{H}_{12}$ as an intermediate compound is suggested by the experiment and first-principle calculations [29,69,70,83]. A pure $\text{CaB}_{12}\text{H}_{12}$ compound has been synthesized and the crystal structure has been determined to be monoclinic with $C2/c$ symmetry [84]. Identification of the intermediate compound is expected to increase our understanding of the dehydrogenation process of $\text{Ca}(\text{BH}_4)_2$. The enthalpy and entropy change for the first step of dehydrogenation are estimated to be $\Delta H = 87 \text{ kJ mol}^{-1} \text{H}_2$ and $\Delta S = 158 \text{ J K}^{-1} \text{mol}^{-1} \text{H}_2$ [80], respectively.

Regarding the rehydrogenation properties of pure $\text{Ca}(\text{BH}_4)_2$, no tangible data are available. $\text{Ca}(\text{BH}_4)_2$ has been predicted theoretically to have limited viability as a reversible storage material for on-board storage due to the formation of a stable intermediate compound of $\text{CaB}_{12}\text{H}_{12}$ [83]. It was found that the ball-milled mixtures of $\text{CaB}_{12}\text{H}_{12}$ and CaH_2 do not produce $\text{Ca}(\text{BH}_4)_2$ during the rehydrogenation test at 670 K in a hydrogen pressure of 100 MPa [84]. With additives, approximately 57% of the $\text{Ca}(\text{BH}_4)_2$ is obtained by rehydrogenation at 623 K in a hydrogen pressure of 10 MPa [85–87].

$\text{Y}(\text{BH}_4)_3$ releases approximately 7.8 mass% of hydrogen when heated to 773 K [88–93]. This value is almost equal to the theoretical dehydrogenation content (7.5 mass%) according to the assumed reaction:



The whole reaction process of $\text{Y}(\text{BH}_4)_3$ on heating to 773 K is summarized as follows: (1) phase transformation, (2) melting, (3) decomposition of $\text{Y}(\text{BH}_4)_3$ into an intermediate compound and YH_3 , (4) decomposition of the intermediate compound, and (5) decomposition of YH_3 into YH_2 [89]. Approximately 1.1–1.3 mass% of hydrogen was rehydrogenated at 573 K in a hydrogen pressure of 35 MPa for 24 h [89]. Similar to that of $\text{Y}(\text{BH}_4)_3$, a multistep dehydrogenation process were also confirmed in $\text{Ce}(\text{BH}_4)_3$ [94]. In addition, there are several other $M(\text{BH}_4)_n$ (e.g., $M = \text{Zn}, \text{Al}, \text{Ti}, \text{Mn}$ and

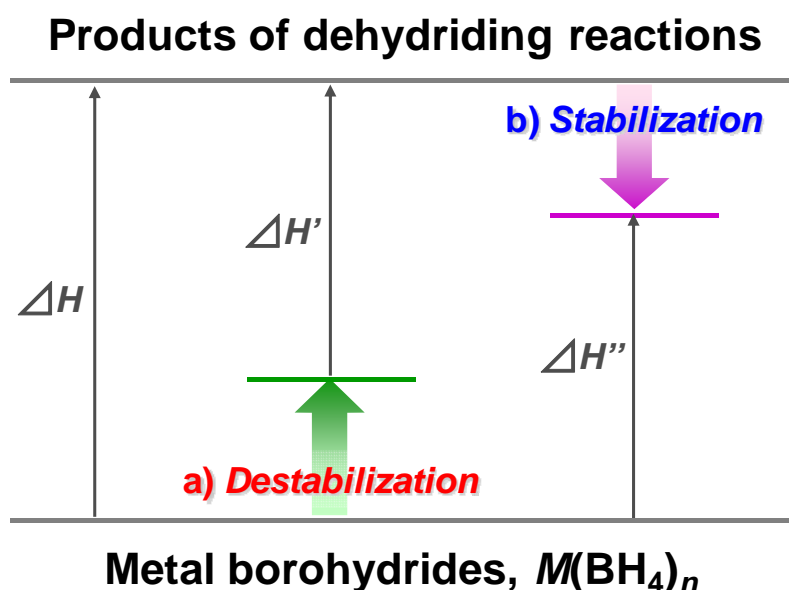
Zr) [95–103]. Most of these were found to be irreversible due to their low melting temperatures and the release of diborane with hydrogen.

3. Improvement of Hydrogen Storage Properties

3.1. Tailoring Thermodynamics

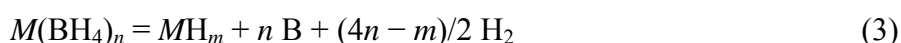
In principle, the Gibbs free energy for a certain reaction determines the reaction temperature. Taking into account that the entropy change ΔS mainly comes from the gaseous hydrogen (*i.e.*, a constant $S_{\text{H}_2}^0 = 130 \text{ J} \cdot \text{K}^{-1} \text{ mol}^{-1} \text{ H}_2$), enthalpy change ΔH becomes the specific indicator to evaluate thermodynamic stability. For metal borohydrides, ΔH is calculated from the difference in the heat of formation between the product and starting materials. Therefore, two main approaches to tailor the thermodynamic stabilities from both sides—the starting materials and products—are expected: (a) destabilization of $M(\text{BH}_4)_n$ and (b) stabilization of dehydrogenation products, as shown in Figure 3.

Figure 3. Schematic illustration of two main approaches to tailor the thermodynamic stabilities of metal borohydrides $M(\text{BH}_4)_n$: (a) destabilization of $M(\text{BH}_4)_n$ and (b) stabilization of dehydrogenation products.



One approach to reducing the enthalpy change ΔH_{deh} is the destabilization of $M(\text{BH}_4)_n$, as illustrated in Figure 3. The thermodynamic stabilities for the series of metal borohydrides $M(\text{BH}_4)_n$ ($M = \text{Li, Na, K, Mg, Ca, Sc, Zr, Hf, Cu, Zn, and Al; } n = 1-4$) have been systematically investigated using first-principles calculations [104]. A good correlation between the predicted heat of formation ΔH_{form} of $M(\text{BH}_4)_n$ and the Pauling electronegativity χ_{P} of M is found, which suggests that the χ_{P} is a useful indicator to estimate the thermodynamic stability of $M(\text{BH}_4)_n$.

The enthalpy change ΔH_{deh} of the dehydrogenation of $M(\text{BH}_4)_n$ correlates not only with the stability of $M(\text{BH}_4)_n$, but also with the stability of the products. The dehydrogenation reactions were assumed as the following equation:



In the case of no MH_m formation, direct decomposition into elements was assumed. Then, the ΔH_{deh} of the dehydrogenation was estimated using the reported values of ΔH_{prod} and predicted ΔH_{form} :

$$\Delta H_{\text{deh}} = \Delta H_{\text{prod}} - \Delta H_{\text{form}} \quad (4)$$

A good correlation between ΔH_{deh} and χ_p was also obtained according to the theoretical prediction. Furthermore, it is expected that $M(\text{BH}_4)_n$ with $\chi_p \geq 1.5$ are thermodynamically unstable [3]. The dehydrogenation properties were experimentally investigated using thermal desorption analysis during the heating process for milling samples [104–106]. A good correlation between T_d (defined as the temperature of the first peak) and χ_p was confirmed experimentally, and was similar to that predicted by the first-principles calculations. Therefore, both the theoretical prediction and the experimental results consistently indicate that T_d can be roughly estimated by considering χ_p as an indicator.

Inspired by this finding, an approach of producing multi cation borohydrides $MM'(\text{BH}_4)_n$, in which M and M' have different electronegativities has been proposed to precisely tailor the thermodynamic stability [107]. Several typical samples has been synthesized, including $\text{LiZr}(\text{BH}_4)_5$, $\text{Li}_2\text{Zr}(\text{BH}_4)_6$, $\text{LiK}(\text{BH}_4)_2$, $\text{LiSc}(\text{BH}_4)_4$, $\text{KSc}(\text{BH}_4)_4$, and so on [107–117]. Note that some samples were reported to form a large $[M'(\text{BH}_4)_n]^{m-}$ complex anion units such as $[\text{Sc}(\text{BH}_4)_4]^-$ [109,117], rather than the bimetallic borohydrides. Most of the $MM'(\text{BH}_4)_n$ exhibit moderate thermodynamic stabilities between $M(\text{BH}_4)_n$ and $M'(\text{BH}_4)_n$. The appropriate combination of cations might be an effective method for adjusting the thermodynamic stability of metal borohydrides, similar to the conventional “alloying” method for hydrogen storage alloys. The detailed dehydrogenation-rehydrogenation properties of the recently synthesized $MM'(\text{BH}_4)_n$ are given in Table 2.

Table 2. Hydrogen storage properties of bimetallic borohydrides, $MM'(\text{BH}_4)_n$.

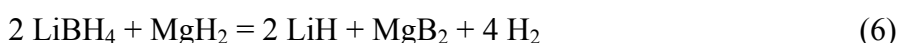
| Borohydrides | Hydrogen (mass%) | | | Conditions: temp (K) [pressure (MPa)] | | Reference |
|---|------------------|-----------------------|----------------|--|----------|-----------|
| | Ideal | Obs (First Dehyd) | Obs (Rehyd) | First Dehyd | Rehyd | |
| $\text{ZrLi}(\text{BH}_4)_5$ | 11.7 | | | 595–873 | | [107] |
| $\text{ZrLi}_2(\text{BH}_4)_6$ | 12.5 | | | 650–873 | | [107] |
| $\text{LiK}(\text{BH}_4)_2$ | 10.6 | | | 653– | | [108] |
| $\text{LiSc}(\text{BH}_4)_4$ | 14.5 | 4.38–6.4 ^m | | 415–673 | 673 [7] | [109,111] |
| $\text{LiZn}_2(\text{BH}_4)_5$ * | 9.5 | | | 238–473 | | [112] |
| $\text{NaZn}_2(\text{BH}_4)_5$ * | 8.8 | | | 241– | | [112] |
| $\text{NaSc}(\text{BH}_4)_4$ | 12.7 | 0.97 ^m | | 440–750 | | [113] |
| $\text{Na}_2\text{Mn}(\text{BH}_4)_4$ | 10.1 | 2.9 | | 393 | | [114] |
| $\text{KSc}(\text{BH}_4)_4$ | 11.2 | 4.4 ^p | | 470–580 | | [117] |
| $\text{LiBH}_4/\text{Mg}(\text{BH}_4)_2$ | 16.0 | 12.5 | 2.5 | 513–773 | 673 [10] | [115] |
| $x\text{LiBH}_4 + (1-x)\text{Ca}(\text{BH}_4)_2$ ($0 < x < 1$) | 9.6–18.5 | 10 (x = 0.4, 0.6) | 4 (x = 0.4) | 473–773 | 673 [9] | [116] |

* represents that the release of B_2H_6 in the decomposition process; ^m indicates the value referred to the mixture of metal borohydride with side products, while ^p indicates the value referred to the pure metal borohydride.

The other approach to reducing enthalpy change ΔH_{deh} is the stabilization of dehydrogenated products by the combination of $M(\text{BH}_4)_n$ with elements, metal hydrides, complex hydrides, and so on. A typical example for this approach is the $2 \text{LiBH}_4 + \text{MgX}$ system [118]. Pure LiBH_4 releases approximately 13.8 mass% of hydrogen according to the following reaction:



The enthalpy and entropy for Equation 5 have been predicted to be $66.6 \text{ kJ mol}^{-1} \text{H}_2$ and $97.4 \text{ J K}^{-1} \text{mol}^{-1}$ [119], respectively, which means T_d (in 0.1 MPa H_2) is approximately 683 K. This temperature is too high for practical applications, although the combination with Mg-based compounds clearly results in a large reduction of ΔH_{deh} . Dehydrogenation of the $\text{LiBH}_4/\text{MgH}_2$ system proceeds as follows:



In this case, due to the formation of MgB_2 , ΔH_{deh} was reduced to $45.8 \text{ kJ mol}^{-1} \text{H}_2$ and T_d (in 0.1 MPa H_2) decreased to approximately 441 K [120]. At the same time, a significant destabilization of LiBH_4 due to combination with the LiNH_2 system was reported [121], as indicated by the much higher dehydrogenation pressure of the combined materials than that of LiBH_4 alone. Due to these significant destabilization effects, a large number of combination materials have been developed. The recent progress on these combination systems [120–185] is summarized in Table 3.

This approach not only reduces the enthalpy of the dehydrogenation, which decreases T_d , but also kinetically enhances the rehydrogenation reaction. That is, in contrast to the formation of pure LiBH_4 (from right to left in Equation 5) discussed in Section 2, LiBH_4 and MgH_2 form simultaneously (from right to left in Equation 6) under fairly moderate conditions: 5 MPa hydrogen pressure in the temperature range 523–573 K [136]. The difference between these two reactions is attributed to the different crystal structures and boron bonding of pure boron and MgB_2 , as shown in Figure 4. That is, in pure boron, the common building blocks are icosahedral units that consist of 12 boron atoms, and each atom is connected to five other atoms via covalent bonds. By contrast, in MgB_2 , each boron atom is connected to a maximum of three other boron atoms. The recent activities of the above-mentioned metal boride systems [136,186–192] are summarized in Table 4.

Figure 4. Schematic illustrations of (a) B_{12} icosahedral unit in boron and (b) layer structure of MgB_2 .

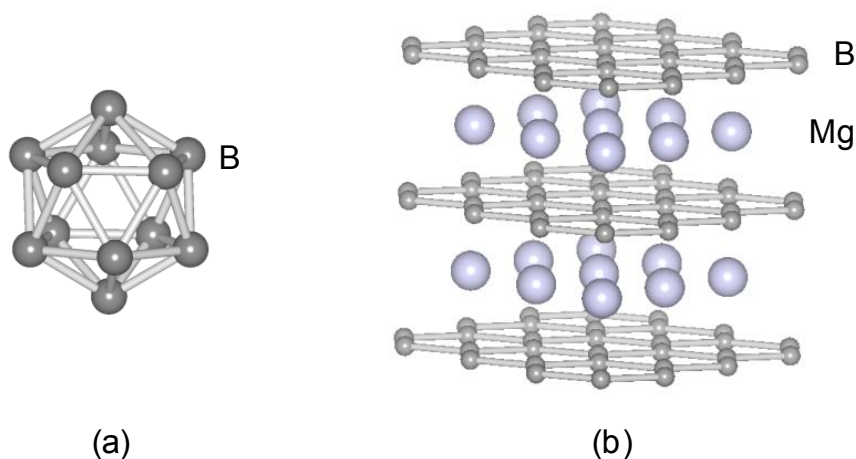


Table 3. Hydrogen storage properties of the combination systems of $M(\text{BH}_4)_n$ with metal hydrides, complex hydrides, metals, *etc.*

| Reaction | Hydrogen (mass%) | | | Conditions: temp (K) [pressure (MPa)] | | Theor/Exp ΔH_{dehyd} (kJ mol ⁻¹ H ₂) | Reference |
|---|------------------|----------------------|----------------|--|----------------------|--|--|
| | Ideal | Obs (First Dehyd) | Obs (Rehyd) | First Dehyd | Rehyd | | |
| $\text{LiBH}_4 + 1/2 \text{MgH}_2 = \text{LiH} + 1/2 \text{MgB}_2 + 2 \text{H}_2$ | 11.5 | 8.0–10.6 | 8.0–10 | 543–723 | 503–723 [10] | T 50.4–66.8/ E 40.5 | [29,120,124, 134–136,142,145,156, 168,172,186] |
| $\text{LiBH}_4 + 2 \text{LiNH}_2 = \text{Li}_3\text{BN}_2 + 4 \text{H}_2$ | 11.9 | 7.8–12 | 0.1 | 622–673 | 573 [5] | E 23 | [121,123,124, 127–130,132,149, 160,166] |
| $\text{LiBH}_4 + 1/2 \text{Al} = \text{LiH} + 1/2 \text{AlB}_2 + 3/2 \text{H}_2$ | 8.6 | 6.8–7.2 | 5–7.6 | 553–823 | 573–773 [10–15.5] | T 18.8–57.9 | [134,135,137,163–165] |
| $\text{LiBH}_4 + 1/2 \text{LiAlH}_4 = 3/2 \text{LiH} + 1/2 \text{AlB}_2 + 9/4 \text{H}_2$ | 11.1 | 6–10 | 4.8–5.1 | 327–773 | 623–873 [4–7] | | [157] |
| $\text{LiBH}_4 + 1/2 \text{Mg} = \text{LiH} + 1/2 \text{MgB}_2 + 3/2 \text{H}_2$ | 8.9 | 5.6 | | 648–773 | | T 46.4 | [134,135] |
| $\text{LiBH}_4 + 1/6 \text{CaH}_2 = \text{LiH} + 1/6 \text{CaB}_6 + 10/6 \text{H}_2$ | 11.7 | 5.1–11.1 | 9–11.1 | 423–773 | 673 [10] | T 45.4–66.5 | [19,135,137,142,144, 168] |
| $\text{LiBH}_4 + 1/2 \text{ScH}_2 = \text{LiH} + 1/2 \text{ScB}_2 + 2 \text{H}_2$ | 8.9 | 4.5 | | 553–723 | | T 34.1 | [134,135,142,143] |
| $\text{LiBH}_4 + 1/6 \text{CeH}_2 = \text{LiH} + 1/6 \text{CeB}_6 + 10/6 \text{H}_2$ | 7.4 | 6.1–6.2 | 6.0 | 443–723 | 623 [10] | T 44.1 | [144,168,177] |
| $\text{LiBH}_4 + 1/4 \text{YH}_3 = \text{LiH} + 1/4 \text{YB}_4 + 15/8 \text{H}_2$ | 8.4 | 7.2 | | 623 | | | [168] |
| $\text{LiBH}_4 + 1/4 \text{MgH}_2 + 1/4 \text{Al} = \text{LiH} + 1/4 \text{MgAlB}_4 + 7/4 \text{H}_2$ | 10.0 | 9.4 | 6 | 533–673 | 673 [4] | E 57 | [159] |
| $\text{Ca}(\text{BH}_4)_2 + \text{MgH}_2 = \text{CaH}_2 + \text{MgB}_2 + 4 \text{H}_2$ | 8.4 | 7.1 | | 623–723 | | T 47 | [135] |

Table 3. Cont.

| | | | | | | | |
|---|------|------|-----|---------|-------------|------|---------------|
| $\text{Ca}(\text{BH}_4)_2 + \text{MgH}_2 = 2/3 \text{CaH}_2 + 1/3 \text{CaB}_6 + \text{Mg} + 13/3 \text{H}_2$ | 9.1 | 8.1 | 5.5 | 593–773 | 623 [9] | T 45 | [187] |
| $\text{Mg}(\text{BH}_4)_2 + \text{LiNH}_2 = \text{Li-Mg} + \text{BN-related} + 5 \text{H}_2$ | 13.1 | 11.4 | | 433–873 | | | [174] |
| $\text{NaBH}_4 + 1/2 \text{MgH}_2 = \text{Na} + 1/2 \text{MgB}_2 + 5/2 \text{H}_2$ | 9.9 | 9 | 6 | 330–723 | 723 [5] | T 62 | [183,186] |
| $\text{NaBH}_4 + 2 \text{NaNH}_2 = \text{Na}_3\text{BN}_2 + 4 \text{H}_2$ * | 7.0 | | | 500–773 | | | [173] |
| $x \text{LiBH}_4 + y (\text{LiNH}_2)_2 + z (\text{MgH}_2) = \text{Li}_3\text{BN}_2 + \text{Mg}_3\text{N}_2 + \text{LiH} + \text{H}_2$ | | | | | | | |
| $x:y:z = 2:1:1$ | 13.0 | 8.5 | 2.9 | 413–743 | 453 [15] | | [140,141,155] |
| 2:0.5:1 | 13.6 | 8.6 | 3.7 | 413–743 | | | |
| 2:1:2 | 11.8 | 6.6 | 3.1 | 428–743 | | | |
| 1:1:1 | 11.3 | 5.6 | 2.7 | 428–743 | | | |
| 3:1:1.5 | 13.4 | 9.1 | | 413–743 | | | |

* represents that the release of NH_3 in the decomposition process: T and E represent the theoretic and experimental values, respectively.

Table 4. Hydrogen storage properties of metal borides and metal hydrides systems.

| Reaction | Hydrogen (mass%) | | | Conditions: temp (K) [pressure (MPa)] | | Reference |
|---|------------------|--------------------|----------------|--|--------------------|---------------------------|
| | Ideal | Obs (First Hyd) | Obs (Dehyd) | First Hyd | Dehyd | |
| $\text{LiH} + 1/2 \text{MgB}_2 + 2 \text{H}_2 = \text{LiBH}_4 + 1/2 \text{MgH}_2$ | 11.5 | 3.2–11 | 3.0–8.0 | 538–673 [9–35] | 538–723 [0–0.6] | [120,145, 182,186,187] |
| $\text{LiF} + 1/2 \text{MgB}_2 + \text{H}_2 = \text{LiBH}_{4-y}\text{F}_y + 1/2 \text{MgF}_2 + \text{LiH}_{1-x}\text{F}_x$ | | 6.6 | 6.4 | 663 [6] | 693 [0.5] | [189] |
| $\text{Li}_7\text{Sn}_2 + 7/2 \text{MgB}_2 + 14 \text{H}_2 = 7 \text{LiBH}_4 + 7/4 \text{Mg}_2\text{Sn} + 1/4 \text{Sn}$ | 5.9 | 2.5–3 | | 573–673 [20–30] | | [186] |
| $\text{CaH}_2 + \text{MgB}_2 + 4\text{H}_2 = \text{Ca}(\text{BH}_4)_2 + \text{MgH}_2$ | 8.4 | 4.7–7 | | 573–673 [20–35] | | [186,187] |
| $\text{NaH} + 1/2 \text{MgB}_2 + 2 \text{H}_2 = \text{NaBH}_4 + 1/2 \text{MgH}_2$ | 7.9 | 6.2–6.7 | | 573–673 [20–35] | | [186] |
| $1/3 \text{CaB}_6 + 2/3 \text{CaH}_2 + 10/3 \text{H}_2 = \text{Ca}(\text{BH}_4)_2$ | 9.6 | 4.8 | | 623 [10] | 543–573 | [186] |
| $2/3 \text{CaH}_2 + 1/3 \text{CaB}_6 + 1/2 \text{Mg} + 23/6 \text{H}_2 = \text{Ca}(\text{BH}_4)_2 + 1/2 \text{MgH}_2$ | 9.3 | | 4.9–5.9 | 623–673 [9] | | [192] |
| $\text{MgNi}_{2.5}\text{B}_2 + 2 \text{LiH} + 4 \text{MgH}_2 + 4\text{H}_2 = 2 \text{LiBH}_4 + 5/2 \text{Mg}_2\text{NiH}_4$ | 2.5 | 1.0 | 1.0 | 623 [16] | 613 [0.4] | [167] |
| $\text{MgB}_2 + 4 \text{H}_2 = \text{Mg}(\text{BH}_4)_2$ | 14.9 | | 11.0 | 673 [95] | | [73,74] |

3.2. Promoting Kinetics

$M(\text{BH}_4)_n$ dehydrogenates via stepwise reactions accompanied by the formation of intermediate compounds. Although the rate-controlling step has not been determined, the complicated dehydrogenation feature makes the promotion of kinetics rather challenging. There are two approaches that have been extensively studied to reduce the reaction barrier: (a) appropriate additives with catalytic abilities and (b) the nanoconfinement approach.

Complex hydrides including alanates, amides, and borohydrides are commonly known to exhibit sluggish kinetics. Since Bogdanovic *et al.* found that the addition of Ti-based compounds significantly promoted the dehydrogenation-rehydrogenation reactions of NaAlH_4 [193], the development of complex hydrides for hydrogen storage has significantly increased. Stimulated by this finding, a large number of additives from oxides, halides, metals, and carbon-based materials to $M(\text{BH}_4)_n$ have been examined [19,20,58,87,101,130,144,150,161,168,170,171,191,194–210]; the corresponding dehydrogenation and rehydrogenation properties are summarized in Table 5. For instance, the most effective additive for LiBH_4 was found to be the mixture of $0.2 \text{ MgCl}_2 + 0.1 \text{ TiCl}_3$, in which approximately 5 mass% of hydrogen was released from 333 K and 4.5 mass% of hydrogen was rehydrogenated at 873 K in 7 MPa H_2 [195]. The addition of TiCl_3 was also proved to be effective for $\text{Mg}(\text{BH}_4)_2$, the starting dehydrogenation temperature of which was reduced to 361 K [58]. Titanium isopropoxide was reported to be an effective additive for the combination system of $2 \text{ LiBH}_4 + \text{MgH}_2$ [136]. According to the X-ray absorption spectroscopy analysis, titanium isopropoxide was demonstrated to form a disordered TiO_2 anatase during ball milling with $2 \text{ LiBH}_4 + \text{MgH}_2$. After several dehydrogenation-rehydrogenation cycles, Ti species were demonstrated to change to Ti_2O_3 and TiB_2 [181]. Similar phenomena were reported for most additives, and the oxidation states of the initial additives vary with cycling experiments, though the catalytic mechanism is still uncertain.

The dehydrogenation-rehydrogenation reactions of $M(\text{BH}_4)_n$ are accompanied by the diffusion of constituent elements such as M , B, and H. The relatively high reaction temperature further prolongs the diffusion distance and enlarges the crystallite size of M and B, thus further degrading the hydrogen storage properties. Fabricating and maintaining the nanosized metal borohydrides is expected to be an effective way to overcome the aforementioned barriers. One known approach is to incorporate hydrogen storage materials into nanoporous materials. It was first applied in the NH_3BH_3 system [211] and good improvement was obtained: The dehydrogenation temperature was largely decreased and the amount of borazine gas (an impurity) was significantly reduced. Recently, this approach was introduced for $M(\text{BH}_4)_n$ materials, and some recent achievements [160,212–222] are summarized in Table 6.

By the incorporation into nanoporous carbon scaffolds with a 13-nm pore size, the dehydrogenation rates of LiBH_4 were found to be up to 50 times faster than those in the bulk materials measured at 573 K [212]. In addition, the capacity loss over three cycles was reduced from 72% for bulk LiBH_4 to ~40% for nanoconfined LiBH_4 . Further, a recent report confirmed the synergetic effects of nanoconfinement and Ni addition on the dehydrogenation and rehydrogenation properties of LiBH_4 . The nanoconfinement of the mixture of LiBH_4 and Ni addition in a nanoporous carbon scaffold shows a higher rehydrogenation rate and larger rehydrogenation amount than those of the samples without Ni addition at 593 K in a hydrogen pressure of 4 MPa [220]. This suggests that the combination of nanoconfinement and additives would be a valid way to improve the hydrogen storage properties of $M(\text{BH}_4)_n$.

Table 5. Hydrogen storage properties of $M(\text{BH}_4)_n$ with additives (oxides, halides, carbon, etc.).

| $M(\text{BH}_4)_n$ | Additives | | Hydrogen (mass%) | | Conditions: temp (K) [pressure (MPa)] | | Toxic Byproduct | Reference |
|--------------------|---|------------------|------------------------|----------------------|--|-------------------|-------------------------------|-------------|
| | Type | Amount | Obs (First Dehyd) | Obs (Rehyd) | First Dehyd | Rehyd | | |
| LiBH ₄ | SiO ₂ | 10–25 mass% | 9–10 ^m | | 423–873 | | | [19,20,204] |
| | TiO ₂ | 25–80 mass% | 4–9 ^m | 3.5–8.3 ^m | 373–873 | 873 [7–10] | | [197,209] |
| | ZrO ₂ | 25 mass% | 8–9 ^m | | 448–873 | | | [197] |
| | V ₂ O ₃ | 25 mass% | 8–9 ^m | 8 ^m | 448–873 | 873 [10] | | [197] |
| | SnO ₂ | 25 mass% | 8–9 ^m | | 448–873 | | | [197] |
| | Nb ₂ O ₅ | 50–80 mass% | 4–6 ^m | | 373–873 | | | [209] |
| | Fe ₂ O ₃ | 50–66.7 mass% | 5.7–9 ^m | | 373–873 | | | [209] |
| | V ₂ O ₅ | 50–66.7 mass% | 5.7–9 ^m | | 373–873 | | | [209] |
| | TiCl ₃ | 10–88 mass% | 2.8–9.2 ^m | 3.4 ^m | 373–873 | 773 [7] | B ₂ H ₆ | [197,208] |
| | CoCl ₂ | 5–100 mol% | 10.5–18.3 ^p | | 503–873 | | B ₂ H ₆ | [213] |
| | TiH ₂ | 10–50 mol% | 6–15 ^m | 2.5–4.5 ^m | 573–873 | 773 [7] | | [208] |
| | TiF ₃ | 10–50 mol% | 6.4–14 ^m | 0.2–4.0 ^m | 373–773 | 623–773 [7–10] | B ₂ H ₆ | [208,211] |
| | ZnF ₂ | 10–50 mol% | 3.7–7 ^m | 1–4 ^m | 393–773 | 773 [7] | B ₂ H ₆ | [208] |
| | mixture of MgCl ₂ /TiCl ₃ | 30 mol% | 5 ^m | 4.5 ^m | 333–873 | 873 [7] | | [198] |
| | Mg | 10–20 mol% | 9 ^m | | 333–873 | | | [198] |
| | Al | 20 mol% | 7.8 ^m | 3.5 ^m | 353–873 | 873 [10] | | [198] |
| | Sc | 33 mol% | 2.9 ^m | | 673–773 | | | [134] |
| Ti | 33 mol% | 2.5 ^m | | 673–773 | | | [134] | |
| V | 33 mol% | 4.4 ^m | | 673–773 | | | [134] | |
| Cr | 33 mol% | 4.4 ^m | | 673–773 | | | [134] | |
| LiBH ₄ | MgH ₂ | 80 mass% | 8.8–9.2 ^m | 8.5 ^m | 627–853 | 673 [10] | | [126,172] |
| | graphite | 30 mass% | 9.9 ^p | 2.6 ^p | 663–773 | 673 [10] | | [212] |
| | activated carbon | 30 mass% | 11.2 ^p | 4.6 ^p | 623–773 | 673 [10] | | [212] |
| | single-walled carbon nanotubes | 30 mass% | 11.4–12.3 ^p | 3.7 ^p | 553–773 | 673 [10] | | [205,212] |
| | single-walled carbon nanotubes | 9.1–50 mass% | 5–11.8 ^p | 3.7–6.1 ^p | 723 (iso) | 673 [10] | | [207] |

Table 5. Cont.

| | | | | | | | | |
|---|---|-------------|-----------------------|----------------------|-----------|-----------|-----------------|-----------|
| | mesoporous carbon | 50 mass% | 7 ^m | 6 ^m | 605–873 | 623 [3] | | [200] |
| | mixture of TiF ₃ /SiO ₂ | 50 mass% | 8.3 ^m | 4 ^m | 343–823 | 773 [4.5] | | [204] |
| | Pt/C | 10–50 mass% | 9.2–15.7 ^m | 6.1 ^m | 553–973 | 873 [3] | | [206] |
| LiBH ₄ + 1/2MgH ₂ | Ti-iso | 5–10 mol% | 6.5–8.4 ^m | 6.0 ^m | 673 (iso) | 623 [5] | | [170,136] |
| | Zr-iso | 10 mol% | 5.5 ^m | | 673 (iso) | | | [150] |
| | ZrCl ₄ | 10 mol% | 7.5 ^m | | 673 (iso) | | | [150] |
| | SiO ₂ | 5 mol% | 9.3 ^m | | 673 (iso) | | | [136] |
| | VCl ₃ | 5 mol% | 9.1 ^m | | 673 (iso) | | | [136] |
| | graphite | 10 mass% | 9.5 ^p | | 723 (iso) | | | [168] |
| | carbon nanofibers | 10 mass% | 10.0 ^p | | 723 (iso) | | | [168] |
| | activated carbon | 10 mass% | 10.0 ^p | | 723 (iso) | | | [168] |
| | single-walled carbon nanotubes | 10 mass% | 10.0 ^p | 6.7 ^p | ~573–773 | 673 [7.5] | | [168] |
| | muti-walled carbon nanotubes | 10 mass% | 10.0 ^p | | 723 (iso) | | | [168] |
| | TiF ₃ | 5 mol% | 9.7 ^p | | 573 (iso) | | | [72] |
| Li ₃ BN ₂ H ₈ | Pt/Vulcan carbon | 1–10 mass% | 9–13 ^m | 1.4 ^m | 388–673 | 423 [8.4] | NH ₃ | [130] |
| | Pd | 5–10 mass% | 11.8–13 ^m | | 473–673 | | | [130] |
| | PdCl ₂ | 8.3 mass% | 10.4 ^m | | 473–673 | | | [130] |
| | CoCl ₂ | 5 mass% | 8–10 ^m | | 388–493 | | | [149] |
| Li ₄ BN ₃ H ₁₀ | NiCl ₂ | 11 mass% | 7.6 ^p | | 433–673 | | NH ₃ | [161] |
| Ca(BH ₄) ₂ + MgH ₂ | Ti-iso | 1 mass% | 7.1 ^m | | 523–723 | | | [190] |
| Ca(BH ₄) ₂ | NbF ₅ | 2 mol% | 8.3 ^m | 4.6–5.0 ^m | ~593–823 | 623 [9] | | [87] |
| | NbCl ₅ | 2 mol% | 4.1–5.0 ^m | 3.1–4.5 ^m | ~593–823 | 623 [9] | | [87] |
| | TiF ₃ | 2 mol% | 4.1–5.0 ^m | 2.5–4.2 ^m | ~593–823 | 623 [9] | | [87] |
| | TiCl ₃ | 2 mol% | 4.1–5.0 ^m | 3.5–4.4 ^m | ~593–823 | 623 [9] | | [87] |
| Mg(BH ₄) ₂ | TiCl ₃ | 25 mass% | 13.7 ^p | | 361–800 | | | [58] |
| | TiO ₂ | 25 mass% | 13.7 ^p | | 483–800 | | | [58] |

^m indicates the value referred to the mixture of metal borohydride with side products, while ^p indicates the value referred to the pure metal borohydride.

Table 6. Hydrogen storage properties of $M(\text{BH}_4)_n$ confined by nanoporous materials.

| Reaction | Type of Nano Scaffold (size (nm)) | Loading Ratio (mass%) | Hydrogen (mass%) | | Conditions: temp (K) [pressure (MPa)] | | Reference |
|---|--------------------------------------|-----------------------|----------------------|------------------|---------------------------------------|----------------|-----------|
| | | | Obs (First Dehyd) | Obs (Rehyd) | First Dehyd | Rehyd | |
| $\text{LiBH}_4 = \text{LiH} + \text{B} + 3/2 \text{H}_2$ | Nanoporous Carbon (13–25) | 25–50 | 4.6–6.4 ^m | | 503–873 | 673 [10] | [212] |
| | Activated carbon (1.75–3.2) | 28.4 | 11.2 ^p | 6.6 ^p | 493–773 | 573 [5] | [213] |
| | Mesoporous carbon (4) | 33 | 3.4 ^m | | 473–773 | | [214] |
| | Nanoporous Carbon (2) | | 8.8 ^p | | 493–673 | | [219] |
| $\text{Li}_3\text{BN}_2\text{H}_8 = \text{Li}_3\text{BN}_2 + 4 \text{H}_2$ * | Nanoporous carbon scaffolds (16 ± 3) | 33 | 11.1 ^p | 3.8 ^p | 523–673 | 573 [5] | [160] |
| | activated carbon AX-21 (2) | 33 | 10.7 ^p | 4.0 ^p | 438–673 | 573 [5] | [160] |
| $\text{Mg}(\text{BH}_4)_2 = \text{MgB}_2 + 4 \text{H}_2$ | Activated carbon (<2) | 44 ± 3 | 6.0 ^m | | 443–773 | | [216] |
| $\text{LiBH}_4 + 3.75 \text{ mass\%Ni}$ | Nanoporous carbon (2–3) | 25 | 14 ^p | 10 ^p | 473–673 | 593 [4] | [220] |
| $\text{LiBH}_4 + 1/2 \text{MgH}_2 = \text{LiH} + 1/2 \text{MgB}_2 + 2 \text{H}_2$ | Nanoporous carbon aerogel (~21) | | 4.7 ^m | 4 ^m | 533–743 | 643–663 [5–10] | [221] |

* represents that the release of NH_3 in the decomposition process; ^m indicates the value referred to the mixture of metal borohydride with side products, while ^p indicates the value referred to the pure metal borohydride.

4. Conclusions

Metal borohydrides $M(\text{BH}_4)_n$ with an extremely high hydrogen density, have been regarded as potential candidates for on-board hydrogen storage. The high reaction temperature and sluggish kinetics, however, decrease their potential for practical applications. In order to overcome these barriers, a number of efforts have been devoted to improving the hydrogen storage properties in both thermodynamic and kinetic areas. The thermodynamic stability of $M(\text{BH}_4)_n$ can be predicted and tailored by considering the electronegativity of M . The multistep reaction pathway together with the formation of an intermediate compound such as $M(\text{B}_{12}\text{H}_{12})_{n/2}$, might account for the high reaction temperature and slow kinetics. The suppression of the formation of $M(\text{B}_{12}\text{H}_{12})_{n/2}$ can be realized by the combination of $M(\text{BH}_4)_n$ with other hydrides or metals. This approach changes the reaction pathway, and therefore, improves the hydrogen storage properties in both thermodynamic and kinetic areas. Regarding the improvement of reaction kinetics, both additives and nanoconfinement have been proved to be vital.

None of the current materials can fulfill the requirements of on-board hydrogen storage for fuel cell vehicles; therefore, continued efforts are required to develop novel materials. According to theoretical predications, many $M(\text{BH}_4)_n$ have the potential to release hydrogen at a moderate temperature, and the sluggish kinetics are considered to be mainly responsible for the high reaction temperature. Effective strategies to achieve fast reaction kinetics will be an important research direction to achieve practical success with metal borohydrides.

Acknowledgments

Financial support received from NEDO (New Energy and Industrial Technology Development Organization, in collaboration with Toyota Central R&D Labs., Inc.); GCOE (Global COE program, Tohoku University); DOE (Department of Energy) and European Commission is greatly appreciated.

References

1. Schlapbach, L.; Züttel, A. Hydrogen-storage materials for mobile applications. *Nature* **2001**, *414*, 353–358.
2. Orimo, S.; Nakamori, Y.; Eliseo, J.; Züttel, A.; Jensen, C.M. Complex Hydrides for Hydrogen Storage. *Chem. Rev.* **2007**, *107*, 4111–4132.
3. Nakamori, Y.; Orimo, S. Borohydrides as hydrogen storage materials. In *Solid-State Hydrogen Storage*; Walker, G., Ed.; Woodhead Publishing Limited: Cambridge, UK, 2008; pp. 420–449.
4. Miwa, K.; Ohba, N.; Towata, S.; Nakamori, Y.; Orimo, S. First-principles Study on Lithium Borohydride LiBH_4 . *Phys. Rev. B* **2004**, *69*, 245120.
5. Ge, Q. Structure and Energetics of LiBH_4 and Its surfaces: A First-Principles Study. *J. Phys. Chem. A* **2004**, *108*, 8682–8690.
6. Vajeeston, P.; Ravindran, P.; Kjekshus, A.; Fjellvåg. Structural Stability of Alkali Boron Tetrahydrides ABH_4 ($A = \text{Li, Na, K, Rb, Cs}$) From First Principle Calculation. *J. Alloys Compd.* **2005**, *387*, 97–104.

7. Łodziana, Z.; Vegge, T. Structural Stability of Complex Hydrides: LiBH_4 Revisited. *Phys. Rev. Lett.* **2004**, *93*, 14550.
8. Orgaz, E.; Membrillo, A.; Castañeda, R.; Aburto, A. Electronic Structure of Ternary Hydrides Based on Light Elements. *J. Alloys Compd.* **2005**, *404–406*, 176–180.
9. Schlesinger, H.I.; Brown, H.C.; Finholt, A.E.; Gilbreath, J.R.; Hoekstra, H.R.; Hyde, E.K. Sodium Borohydride, Its Hydrolysis and its Use as a Reducing Agent and in the Generation of Hydrogen. *J. Am. Chem. Soc.* **1953**, *75*, 215–219.
10. Liu, B.H.; Li, Z.P.; Suda, S. Nickel- and cobalt-based catalysts for hydrogen generation by hydrolysis of borohydride. *J. Alloys Compd.* **2006**, *415*, 288–293.
11. Wang, P.; Kang, X.D. Hydrogen-rich boron-containing materials for hydrogen storage. *Dalton Trans.* **2008**, *40*, 5400–5413.
12. Grochala, W.; Edwards, P.P. Thermal Decomposition of the Non-Interstitial Hydrides for the Storage and Production of Hydrogen. *Chem. Rev.* **2004**, *104*, 1283–1315.
13. Sakintuna, B.; Lamari-Darkrimb, F.; Hirscherc, M. Metal Hydride Materials for Solid Hydrogen Storage: A review. *Int. J. Hydrogen Energy* **2007**, *32*, 1121–1140.
14. Chen, P.; Zhu, M. Recent progress in hydrogen storage. *Mater. Today.* **2008**, *11*, 36–43.
15. Rönnebro, E. Development of group II borohydrides as hydrogen storage materials. *Curr. Opin. Solid State Mater. Sci.* **2010**, doi:10.1016/j.cossms.2010.10.003.
16. George, L.; Saxena, S.K. Structural Stability of Metal Hydrides, Alanates and Borohydrides of Alkali and Alkali-Earth Elements: A Review. *Int. J. Hydrogen Energy* **2010**, *35*, 5454–5470.
17. Jain, I.P.; Jain P.; Jain, A. Novel hydrogen storage materials: A review of lightweight complex hydrides. *J. Alloys Compd.* **2010**, *503*, 303–339.
18. Hagemann H.; Černý, R. Synthetic approaches to inorganic borohydrides. *Dalton Trans.* **2010**, *39*, 6006–6012.
19. Züttel, A.; Wenger, P.; Rentsch, S.; Sudan, P. LiBH_4 A New Hydrogen Storage Material. *J. Power Sources* **2003**, *118*, 1–7.
20. Züttel, A.; Rentsch, S.; Fischer, P.; Wenger, P.; Sudan, P.; Mauron, Ph.; Emmenegger, Ch. Hydrogen Storage Properties of LiBH_4 . *J. Alloys Compd.* **2003**, *356–357*, 515–520.
21. Nakamori, Y.; Orimo, S. Destabilization of Li-based Complex Hydrides. *J. Alloys Compd.* **2004**, *370*, 271–275.
22. Orimo, S.; Nakamor, Y.; Züttel, A. Material Properties of MBH_4 (M = Li, Na, and K). *Mater. Sci. Eng. B* **2004**, *108*, 51–53.
23. Orimo, S.; Nakamori, Y.; Kitahara, G.; Miwa, K.; Ohba, N.; Towata, S.; Züttel, A. Dehydriding and Rehydriding Reactions of LiBH_4 . *J. Alloys Compd.* **2005**, *404–406*, 427–430.
24. Nakamori, Y.; Orimo, S.; Tsutaoka, T. Dehydriding Reaction of Metal Hydrides and Alkali Borohydrides Enhanced by Microwave Irradiation. *Appl. Phys. Lett.* **2006**, *88*, 112104.
25. Züttel, A.; Borgschulte, A.; Orimo, S. Tetrahydroborates as New Hydrogen Storage Materials. *Scripta Mater.* **2007**, *56*, 823–828.
26. Orimo, S.; Nakamori, Y.; Ohba, N.; Miwa, K.; Aoki, M.; Miwa, S.; Züttel, A. Experimental Studies on Intermediate Compound of LiBH_4 . *Appl. Phys. Lett.* **2006**, *89*, 021920.

27. Ohba, N.; Miwa, K.; Aoki, M.; Noritake, T.; Towata, S.; Nakamori, Y.; Orimo, S.; Züttel, A. First-Principles Study on the Stability of Intermediate Compounds of LiBH_4 . *Phys. Rev. B* **2006**, *74*, 075110.
28. Hwang, S.-J.; Bowman, R.C., Jr.; Reiter, J.W.; Rijssenbeek, J.; Soloverchik, G.L.; Zhao, J.-C.; Kabbour, H.; Ahn, C.C. NMR Confirmation for Formation of $[\text{B}_{12}\text{H}_{12}]^{2-}$ Complexes during Hydrogen Desorption from Metal Borohydrides. *J. Phys. Chem. C* **2008**, *112*, 3164–3169.
29. Ozolin, V.; Majzoub, E.H.; Wolverton, C. First-Principles Prediction of Thermodynamically Reversible Hydrogen Storage Reactions in the Li-Mg-Ca-B-H. System. *J. Am. Chem. Soc.* **2009**, *131*, 230–237.
30. Her, J.-H.; Yousufuddin, M.; Zhou, W.; Jalisatgi, S.S.; Kulleck, J.G.; Zan, J.A.; Hwang, S.-J.; Bowman, R.C., Jr.; Udovic, T.J. Crystal Structure of $\text{Li}_2\text{B}_{12}\text{H}_{12}$: A Possible Intermediate Phase in the Decomposition of LiBH_4 . *Inorg. Chem.* **2008**, *47*, 9757–9759.
31. Friedrichs, O.; Remhof, A.; Hwang, S.-J.; Züttel, A. Role of $\text{Li}_2\text{B}_{12}\text{H}_{12}$ for the Formation and Decomposition of LiBH_4 . *Chem. Mater.* **2009**, *22*, 3265–3268.
32. Soulié, J-Ph.; Renaudin, G.; Černý, R.; Yvon, K. Lithium Boro-hydride LiBH_4 . I. Crystal Structure. *J. Alloys Compd.* **2002**, *346*, 200–205.
33. Renaudin, G.; Gomes, S.; Hagemann, H.; Keller, L.; Yvon, K. Structural and Spectroscopic Studies on the Alkali Borohydrides MBH_4 (M = Na, K, Rb, Cs). *J. Alloys Compd.* **2004**, *375*, 98–106.
34. Frankcombe, T.J.; Kroes, G.-J. Quasiharmonic Approximation Applied to LiBH_4 and Its Decomposition Products. *Phys. Rev. B* **2006**, *73*, 174302.
35. Hartman, M.R.; Rush, J.J.; Udovic, T.J.; Bowman, R.C., Jr.; Hwang, S.-J. Structure and Vibrational Dynamics of Isotopically Labeled Lithium Borohydride Using Neutron Diffraction and Spectroscopy. *J. Solid State Chem.* **2007**, *180*, 1298–1305.
36. Łodziana, Z.; Züttel, A.; Zielinski, P. Titanium and Native Defects in LiBH_4 and NaAlH_4 . *J. Phys.: Condens. Matter.* **2008**, *20*, 465210.
37. Borgschulte, A.; Züttel, A.; Hug, P.; Racu, A.-M.; Schoenes, J. Hydrogen-Deuterium Exchange in Bulk LiBH_4 . *J. Phys. Chem. A* **2008**, *112*, 4749–4753.
38. Buchter, F.; Łodziana, Z.; Mauron, Ph.; Remhof, A.; Friedrichs, Q.; Borgschulte, A.; Züttel, A.; Sheptyakov, D.; Strässle, Th.; Ramirez-Cuesta, A.J. Dynamical Properties and Temperature Induced Molecular Disordering of LiBH_4 and LiBD_4 . *Phys. Rev. B* **2008**, *78*, 094302.
39. Skripov, A.V.; Soloninin, A.V.; Filinchuk, Y.; Chernyshov, D. Nuclear Magnetic Resonance Study of Rotational Motion and The Phase transition in LiBH_4 . *J. Phys. Chem. C* **2008**, *112*, 18701–18705.
40. Corey, R.L.; Shane, D.T.; Bowman, R.C., Jr.; Conradi, M.S. Atomic Motions in LiBH_4 by NMR. *J. Phys. Chem. C* **2008**, *112*, 18706–18710.
41. Gremaud, R.; Łodziana, Z.; Hug, P.; Willenberg, B.; Racu, A.-M.; Schoenes, J.; Ramirez-Cuesta, A.J.; Clark, S.J.; Refson, K.; Züttel, A.; Borgschulte, A. Evidence for Hydrogen Transport in Deuterated LiBH_4 from Low-Temperature Raman-Scattering Measurement and First-Principles Calculations. *Phys. Rev. B* **2008**, *80*, 100301.
42. Filinchuk, Y.; Chernyshov, D.; Nevidomskyy, A.; Dmitriev, V. High-Pressure Polymorphism as a Step towards Destabilization of LiBH_4 . *Angew. Chem. Int. Ed.* **2008**, *47*, 529–532.

43. Shane, D.T.; Bowman, R.C., Jr.; Conradi, M.S. Exchange of Hydrogen Atoms between BH_4 in LiBH_4 . *J. Phys. Chem. C* **2009**, *113*, 5039–5042.
44. Ramzan, M.; Ahuja, R. *Ab initio* Molecular Dynamics Study of the Hydrogen-Deuterium Exchange in Bulk Lithiumborohydride (LiBH_4). *Appl. Phys. Lett.* **2009**, *94*, 141903.
45. Hagemann, H.; Filinchuk, Y.; Chernyshov, D.; van Beek, W. Lattice Anharmonicity and Structural Evolution of LiBH_4 : an Insight from Raman and X-ray Diffraction Experiments. *Phase Transitions* **2009**, *82*, 344–355.
46. Andresen, E.R.; Gremaud, R.; Borgschulte, A.; Ramirez-Cuesta, A.J.; Züttel, A.; Hamm, P. Vibrational Dynamics of LiBH_4 by Infrared Pump-Probe and 2D Spectroscopy. *J. Phys. Chem. A* **2009**, *113*, 12838–12846.
47. Hao, S.; Sholl, D.S. The Role of Interstitial H_2 in Hydrogen Diffusion in Light Metal Borohydrides. *Phys. Chem. Chem. Phys.* **2009**, *11*, 11106–11109.
48. Galvez-Ruiz, J.C.; Sanchez, M. Structural Analysis of Alkali Metal Tetrahydroborates: The Role of Metal and Coordination from in the $[\text{BH}_4]^-$ Anion Structure. *J. Mol. Struct.: Theochem.* **2009**, *908*, 114–116.
49. Remhof, A.; Gremaud, R.; Buchter, F.; Lodziana, Z.; Embs, J.P.; Ramirez-Cuesta, A.J.; Borgschulte, A.; Züttel, A. Hydrogen Dynamics in Lightweight Tetrahydroborates. *Z. Phys. Chem.* **2010**, *224*, 263–278.
50. Remhof, A.; Lodziana, Z.; Martelli, P.; Friedrichs, O.; Züttel, A.; Skripov, A.V.; Embs, J.P.; Strässle, T. Rotational Motion of BH_4 Units in MBH_4 ($\text{M} = \text{Li}, \text{Na}, \text{K}$) from Quasielastic Neutron Scattering and Density Functional Calculations. *Phys. Rev. B* **2010**, *81*, 214304.
51. Mauron, P.; Buchter, F.; Friedrichs, O.; Remhof, A.; Biemann, M.; Zwicky, C.N.; Züttel, A. Stability and Reversibility of LiBH_4 . *J. Phys. Chem. B* **2008**, *112*, 906–910.
52. Friedrichs, O.; Buchter, F.; Borgschulte, A.; Remhof, A.; Zwicky, C.N.; Mauron, P.H.; Biemann, M.; Züttel, A. Direct Synthesis of $\text{Li}[\text{BH}_4]$ and $\text{Li}[\text{BD}_4]$ from the Elements. *Acta Mater.* **2007**, *56*, 949–954.
53. Remhof, A.; Friedrichs, O.; Buchter, F.; Mauron, P.H.; Züttel, A.; Wallacher, D. Solid-State Synthesis of LiBD_4 Observed by In Situ Neutron Diffraction. *Phys. Chem. Chem. Phys.* **2008**, *10*, 5859–5862.
54. Friedrichs, O.; Borgschulte, A.; Kato, S.; Buchter, F.; Gremaud, R.; Remhof, A.; Züttel, A. Low-Temperature Synthesis of LiBH_4 by Gas-Solid Reaction. *Chem. Eur. J.* **2009**, *15*, 5531–5534.
55. Friedrichs, O.; Remhof, A.; Borgschulte, A.; Buchter, F.; Orimo, S.; Züttel, A. Breaking the passivation—the road to a solvent free borohydride synthesis. *Phys. Chem. Chem. Phys.* **2010**, *12*, 10919–10922.
56. Matsunaga, T.; Buchter, F.; Mauron, P.; Biemann, M.; Nakamori, Y.; Orimo, S.; Ohba, N.; Miwa, K.; Towata, S.; Züttel, A. Hydrogen Storage Properties of $\text{Mg}(\text{BH}_4)_2$. *J. Alloys Compd.* **2008**, *459*, 583–588.
57. Chłopek, K.; Frommen, C.; Léon, A.; Zabara, O.; Fichtner, M. Synthesis and Properties of Magnesium Tetrahydroborate, $\text{Mg}(\text{BH}_4)_2$. *J. Mater. Chem.* **2007**, *17*, 3496–3503.
58. Li, H.-W.; Kikuchi, K.; Nakamori, Y.; Miwa, K.; Towata, S.; Orimo, S. Effects of Ball Milling and Additives on Dehydrogenating Behaviors of Well-crystallized $\text{Mg}(\text{BH}_4)_2$. *Scripta Mater.* **2007**, *57*, 679–682.

59. Riktor, M.D.; Sørby, M.H.; Chłopek, K.; Fichtner, M.; Buchter, F.; Züttel, A.; Hauback, B.C. In Situ Synchrotron Diffraction Studies of Phase Transitions and Thermal Decomposition of $\text{Mg}(\text{BH}_4)_2$ and $\text{Ca}(\text{BH}_4)_2$. *J. Mater. Chem.* **2007**, *17*, 4939–4942.
60. Matsunaga, T.; Buchter, F.; Miwa, K.; Towata, S.; Orimo, S.; Züttel, A. Magnesium borohydride: A New Hydrogen Storage Material. *Renew. Energy* **2008**, *33*, 193–196.
61. Varin, R.A.; Chiu, Ch.; Wronski, Z.S. Mechano-Chemical Activation Synthesis (MCAS) of Disordered $\text{Mg}(\text{BH}_4)_2$ Using NaBH_4 . *J. Alloys Compd.* **2008**, *462*, 201–208.
62. Li, H.-W.; Kikuchi, K.; Nakamori, Y.; Ohba, N.; Miwa, K.; Towata, S.; Orimo, S. Dehydrogenating and Rehydrogenating Processes of Well-Crystallized $\text{Mg}(\text{BH}_4)_2$ Accompanying with Formation of Intermediate Compounds. *Acta Mater.* **2008**, *56*, 1342–1347.
63. Hanada, N.; Chłopek, K.; Frommen, C.; Lohstroh, W.; Fichtner, M. Thermal Decomposition of $\text{Mg}(\text{BH}_4)_2$ Under He flow and H_2 Pressure. *J. Mater. Chem.* **2008**, *18*, 2611–2614.
64. Yan, Y.; Li, H.-W.; Nakamori, Y.; Ohba, N.; Miwa, K.; Towata, S.; Orimo, S. Differential Scanning Calorimetry Measurements of Magnesium Borohydride $\text{Mg}(\text{BH}_4)_2$. *Mater. Trans.* **2008**, *49*, 2751–2752.
65. Soloveichika, G.L.; Gao, Y.; Rijssenbeek, J.; Andrus, M.; Kniajanski, S.; Bowman, R.C., Jr.; Hwang, S.-J.; Zhao, J.-C. Magnesium Borohydride as a Hydrogen Storage Material: Properties and Dehydrogenation Pathway of Unsolvated $\text{Mg}(\text{BH}_4)_2$. *Int. J. Hydrogen Energy* **2009**, *34*, 916–928.
66. Li, H.-W.; Miwa, K.; Ohba, N.; Fujita, T.; Sato, T.; Yan, Y.; Towata, S.; Chen, M.W.; Orimo, S. Formation of Intermediate Compound with $\text{B}_{12}\text{H}_{12}$ Cluster: Experimental and Theoretical Studies on Magnesium Borohydride $\text{Mg}(\text{BH}_4)_2$. *Nanotechnology* **2009**, *20*, 204013.
67. Ozolins, V.; Majzoub, E.H.; Wolverton, C. First-Principles Prediction of a Ground State Crystal Structure of Magnesium Borohydride. *Phys. Rev. Lett.* **2008**, *100*, 135501.
68. van Setten, M.J.; Lohstroh, W.; Fichtner, M. A New Phase in the Decomposition of $\text{Mg}(\text{BH}_4)_2$: First-Principles Simulated Annealing. *J. Mater. Chem.* **2009**, *19*, 7081–7087.
69. Kulkarni, A.D.; Wang, L.L.; Johnson, D.D.; Sholl, D.S.; Johnson, J.K. First-principles Characterization of Amorphous Phases of $\text{MB}_{12}\text{H}_{12}$, $\text{M} = \text{Mg}, \text{Ca}$. *J. Phys. Chem. C* **2010**, *114*, 14601–14605.
70. Li, S.; Willis, M.; Jena, P. Reaction Intermediates during the Dehydrogenation of Metal Borohydrides: A Cluster Perspective. *J. Phys. Chem. C* **2010**, *114*, 16849–16854.
71. Chen, X.; Lingam, H.K.; Huang, Z.; Yisgedu, T.; Zhao, J.-C.; Shore, S.G. Thermal Decomposition Behavior of Hydrated Magnesium Dodecahydrododecaborates. *J. Phys. Chem. Lett.* **2010**, *1*, 201–204.
72. Newhouse, R.J.; Stavila, V.; Hwang, S.-J.; Klebanoff, L.E.; Zhang, J.Z. Reversibility and Improved Hydrogen Release of Magnesium Borohydride. *J. Phys. Chem. C* **2010**, *114*, 5224–5232.
73. Severa, G.; Rönnebro, E.; Jensen, C.M. Direct Hydrogenation of Magnesium Boride to Magnesium Borohydride: Demonstration of >11 Weight Percent Reversible Hydrogen Storage. *Chem. Commun.* **2010**, *46*, 421–423.
74. Li, H.-W.; Matsunaga, T.; Yan, Y.; Maekawa, H.; Ishikiriyama, M.; Orimo, S. Nanostructure-induced hydrogenation of layered compound MgB_2 . *J. Alloys Compd.* **2010**, *505*, 654–656.

75. Pistidda, C.; Garroni, S.; Dolci, F.; Bardají, E.G.; Khandelwal, A.; Nolis, P.; Dornheim, M.; Gosalawit, R.; Jensen, T.; Cerenius, Y.; Suriñach, S.; Baró, M.D.; Lohstroh, W.; Fichtner, M. Synthesis of amorphous $\text{Mg}(\text{BH}_4)_2$ from MgB_2 and H_2 at room temperature. *J. Alloys Compd.* **2010**, *508*, 212–215.
76. Chong, M.; Karkamkar, A.; Autrey, T.; Orimo, S.; Jalisatgi, S.; Jensen, C.M. Reversible dehydrogenation of magnesium borohydride to magnesium triborane in the solid state under moderate conditions. *Chem. Commun.* **2011**, *47*, 1330–1332.
77. Miwa, K.; Aoki, M.; Noritake, T.; Ohba, N.; Nakamori, Y.; Towata, S.; Züttel, A.; Orimo, S. Thermodynamical Stability of Calcium Borohydride $\text{Ca}(\text{BH}_4)_2$. *Phys. Rev. B* **2006**, *74*, 155122.
78. Kim, J.-H.; Jin, S.-A.; Shim, J.-H.; Cho, Y.W. Thermal Decomposition Behavior of Calcium Borohydride $\text{Ca}(\text{BH}_4)_2$. *J. Alloys Compd.* **2008**, *461*, L20–L22.
79. Aoki, M.; Miwa, K.; Noritake, T.; Ohba, N.; Matsumoto, M.; Li, H.-W.; Nakamori, Y.; Towata, S.; Orimo, S. Structural and Dehydrogenation Properties of $\text{Ca}(\text{BH}_4)_2$. *Appl. Phys. A* **2008**, *92*, 601–605.
80. Mao, J.; Guo, Z.; Poh, C.K.; Ranjbar, A.; Guo, Y.; Yu, X.; Liu, H. Study on the dehydrogenation kinetics and thermodynamics of $\text{Ca}(\text{BH}_4)_2$. *J. Alloys Compd.* **2010**, *500*, 200–205.
81. Riktor, M.D.; Sørby, M.H.; Chopek, K.; Fichtner, M.; Haubac, B.C.; The Identification of a Hitherto Unknown Intermediate Phase CaB_2H_x from Decomposition of $\text{Ca}(\text{BH}_4)_2$. *J. Mater. Chem.* **2009**, *19*, 2754–2759.
82. Frankcombe, T.J. Calcium Borohydride for Hydrogen Storage: A Computational Study of $\text{Ca}(\text{BH}_4)_2$ Crystal Structures and the CaB_2H_x Intermediate. *J. Phys. Chem. C* **2010**, *114*, 9503–9509.
83. Wang, L.-L.; Graham, D.D.; Robertson, I.M.; Johnson, D.D. On the Reversibility of Hydrogen-Storage Reactions in $\text{Ca}(\text{BH}_4)_2$: Characterization via Experiment and Theory. *J. Phys. Chem. C* **2009**, *113*, 20088–20096.
84. Stavila, V.; Her, J.-H.; Zhou, W.; Hwang, S.-J.; Kim, C.; Ottley, L.A.M.; Udovic, T.J. Probing the structure, stability and hydrogen storage properties of calcium dodecahydro-closedodecaborate. *J. Solid State Chem.* **2010**, *183*, 1133–1140.
85. Rönnebro, E.; Majzoub, E.H. Calcium Borohydride for Hydrogen Storage: Catalysis and Reversibility. *J. Phys. Chem. B* **2007**, *111*, 12045–12047.
86. Kim, J.-H.; Jin, S.-A.; Shim, J.-H.; Cho, Y.W. Reversible Hydrogen Storage in Calcium Borohydride $\text{Ca}(\text{BH}_4)_2$. *Scripta Mater.* **2008**, *58*, 481–483.
87. Kim, J.-H.; Shim, J.-H.; Cho, Y.W. On the Reversibility of Hydrogen Storage in Ti- and Nb-catalyzed $\text{Ca}(\text{BH}_4)_2$. *J. Power Sources.* **2008**, *181*, 140–143.
88. Sato, T.; Miwa, K.; Nakamori, Y.; Ohoyama, K.; Li, H.-W.; Noritake, T.; Aoki, M.; Towata, S.; Orimo, S. Experimental and computational studies on solvent-free rare-earth metal borohydrides $\text{R}(\text{BH}_4)_3$ ($\text{R} = \text{Y}, \text{Dy}, \text{and Gd}$). *Phys. Rev. B* **2008**, *77*, 104114.
89. Yan, Y.; Li, H.-W.; Sato, T.; Umeda, N.; Miwa, K.; Towata, S.; Orimo, S. Dehydrogenation and rehydrogenation properties of yttrium borohydride $\text{Y}(\text{BH}_4)_3$ prepared by liquid-phase synthesis. *Int. J. Hydrogen Energy* **2009**, *34*, 5732–5736.

90. Frommen, C.; Aliouane, N.; Deledda, S.; Fonnelop, J.E.; Grove, H.; Lieutenant, K.; Llamas-Jansa, I.; Sartori, S.; Sorby, M.H.; Hauback, B.C. Crystal structure, polymorphism, and thermal properties of yttrium borohydride $Y(BH_4)_3$. *J. Alloys Compd.* **2010**, *496*, 710–716.
91. Ravnsbæk, D.B.; Filinchuk, Y.; Cerny, Radovan.; Ley, M.B.; Haase, D.; Jakobsen, H.J.; Skibsted, J.; Jensen T.R. Thermal Polymorphism and Decomposition of $Y(BH_4)_3$. *Inorg. Chem.* **2010**, *49*, 3801–3809.
92. Lee, Y.-S.; Shim, J.-H.; Cho, Y.W. Polymorphism and Thermodynamics of $Y(BH_4)_3$ from First Principles. *J. Phys. Chem. C* **2010**, *114*, 12833–12837.
93. Jaroń, T.; Grochala, W. $Y(BH_4)_3$ —an Old–New Ternary Hydrogen Store aka Learning from a Multitude of Failures. *Dalton Trans.* **2010**, *39*, 160–166.
94. Gennari, F.C.; Esquivel, M.R. Synthesis and Dehydriding Process of Crystalline $Ce(BH_4)_3$. *J. Alloys Compd.* **2009**, *485*, L47–L51.
95. Jeon, E.; Cho, Y.W. Mechanochemical Synthesis and Thermal Decomposition of Zinc Borohydride. *J. Alloys Compd.* **2006**, *422*, 273–275.
96. Srinivasan, S.; Escobar, D.; Jurczyk, M.; Goswami, Y.; Stefanakos, E. Nanocatalyst Doping of $Zn(BH_4)_2$. *J. Alloys Compd.* **2008**, *462*, 294–302.
97. Titov, L.V.; Eremin, E.R. Complex of Aluminum Borohydride with Calcium Borohydride. *Russ. Chem. B.* **1975**, *24*, 1095–1096.
98. Fang, Z.Z.; Ma, L.P.; Kang, X.D.; Wang, P.J.; Wang, P.; Cheng, H.M. *In situ* Formation and Rapid Decomposition of $Ti(BH_4)_3$ by Mechanical Milling $LiBH_4$ with TiF_3 . *Appl. Phys. Lett.* **2009**, *94*, 044104.
99. Gennari, F.C.; Albanesi, L.F.; Rios, I.J. Synthesis and Thermal Stability of $Zr(BH_4)_4$ and $Zr(BD_4)_4$ Produced by Mechanochemical Processing. *Inorg. Chim. Acta.* **2009**, *362*, 3731–3737.
100. Łodziana, Z. Multivalent metal tetrahydroborides of Al, Sc, Y, Ti, and Zr. *Phy. Rev. B* **2010**, *81*, 144108.
101. Choudhury, P.; Srinivasan, S.S.; Bhethanabotla, V.R.; Goswami, Y.; McGrath, K.; Stefanakos, E.K. Nano-Ni Doped Li-Mn-B-H System as a New Hydrogen Storage Candidate. *Int. J. Hydrogen Energy.* **2009**, *34*, 6325–6334.
102. Varin, R.A.; Zbroniec, L. The Effects of Ball Milling Nanometric Nickel on the Hydrogen Desorption from Lithium Borohydride and Manganese Chloride ($3 LiBH_4 + MnCl_2$) Mixture. *Int. J. Hydrogen Energy.* **2010**, *35*, 3588–3597.
103. Černý, R.; Penin, N.; Hagemann, H.; Filinchuk Y. The First Crystallographic and Spectroscopic Characterization of a 3d-Metal Borohydride: $Mn(BH_4)_2$. *J. Phys. Chem. C* **2009**, *113*, 9003–9007.
104. Nakamori, Y.; Miwa, K.; Ninoyiya, A.; Li, H.; Ohba, N.; Towata, S.; Züttel, A.; Orimo, S. Correlation between Thermodynamical Stabilities of Metal Borohydrides and Cation Electronegativities: First-Principles Calculations and Experiments. *Phys. Rev. B* **2006**, *74*, 045126.
105. Nakamori, Y.; Li, H.-W.; Mastuo, M.; Miwa, K.; Towata, S.; Orimo, S. Development of Metal Borohydrides for Hydrogen Storage. *J. Phys. Chem. Sol.* **2008**, *69*, 2292–2296.
106. Sugiyama, J.; Ikedo, Y.; Noritake, T.; Ofer, O.; Goko, T.; Månsson, M.; Miwa, K.; Ansaldo, E.J.; Brewer, J.H.; Chow, K.H.; Towata, S. Microscopic Indicator for Thermodynamic Stability of

- Hydrogen Storage Materials Provided by Positive Muon-Spin Rotation. *Phys. Rev. B* **2010**, *81*, 092103.
107. Li, H.-W.; Orimo, S.; Nakamori, Y.; Miwa, K.; Ohba, N. Towata, S.; Züttel, A. Materials Designing of Metal Borohydrides: Viewpoints from Thermodynamically Stabilities. *J. Alloys Compd.* **2007**, *446–447*, 315–318.
 108. Nickels, E.A.; Jones, M.O.; David, W.I.F.; Johnson, S.R.; Lowton, R.L.; Sommariva, M.; Edwards, P.P. Tuning the Decomposition Temperature in Complex Hydrides: Synthesis of a Mixed Alkali Metal Borohydride. *Angew. Chem. Int. Ed.* **2008**, *47*, 2817–2819.
 109. Hagemann, H.; Longhini, M.; Kaminski, J.W.; Wesolowski, T.A.; Černý, R.; Penin, N.; Sørby, M.H.; Hauback, B.C.; Severa, G.; Jensen, C.M. $\text{LiSc}(\text{BH}_4)_4$: A Novel Salt of Li^+ and Discrete $\text{Sc}(\text{BH}_4)_4^-$ Complex Anions. *J. Phys. Chem. A* **2008**, *112*, 7551–7555.
 110. Seballos, J.; Zhang, J.Z.; Rönnebro, E.; Herberg, J.L.; Majzoub, E.H. Metastability and Crystal Structure of the Bialkali Complex Metal Borohydride $\text{NaK}(\text{BH}_4)_2$. *J. Alloys Compd.* **2009**, *476*, 446–450.
 111. Kim, C.; Hwang, S.-J.; Bowman, R.C., Jr.; Reiter, J.W.; Zan, J.A.; Kulleck, J.G.; Kabbour, H.; Majzoub, E.H.; Ozolins, V. $\text{LiSc}(\text{BH}_4)_4$ as a Hydrogen Storage Material: Multinuclear High-Resolution Solid-State NMR and First-Principles Density Functional Theory Studies. *J. Phys. Chem. C* **2009**, *113*, 9956–9968.
 112. Ravnsbæk, D.; Filinchuk, Y.; Cerenius, Y.; Jakobsen, H.J.; Besenbacher, F.; Skibsted, J.; Jensen, T.R. A Series of Mixed-Metal Borohydrides. *Angew. Chem. Int. Ed.* **2009**, *48*, 6659–6663.
 113. Černý, R.; Severa, G.; Ravnsbæk, D.B.; Filinchuk, Y.; D’Anna, V.; Hagemann, H.; Haase, D.; Jensen, C.M.; Jensen, T.R. $\text{NaSc}(\text{BH}_4)_4$: A Novel Scandium-Based Borohydride. *J. Phys. Chem. C* **2010**, *114*, 1357–1364.
 114. Severa, G.; Hagemann, H.; Longhini, M.; Kaminski, J.W.; Wesolowski, T.A.; Jensen, C.M. Thermal Desorption, Vibrational Spectroscopic, and DFT Computational Studies of the Complex Manganese Borohydrides $\text{Mn}(\text{BH}_4)_2$ and $[\text{Mn}(\text{BH}_4)_4]^{2-}$. *J. Phys. Chem. C* **2010**, *114*, 15516–15521.
 115. Fang, Z.Z.; Kang, X.D.; Wang, P.; Li, H.-W.; Orimo, S. Unexpected Dehydrogenation Behavior of $\text{LiBH}_4/\text{Mg}(\text{BH}_4)_2$ Mixture Associated with the In Situ Formation of Dual-Cation Borohydride. *J. Alloys Compd.* **2010**, *491*, L1–L4.
 116. Lee, J.Y.; Ravnsbæk, D.; Lee, Y.-S.; Kim, Y.; Cerenius, Y.; Shim, J.-H.; Jensen, T.R.; Hur, N.H.; Cho, Y.W. Decomposition Reactions and Reversibility of the $\text{LiBH}_4\text{-Ca}(\text{BH}_4)_2$ Composite. *J. Phys. Chem. C* **2009**, *113*, 15080–15086.
 117. Černý, R.; Ravnsbæk, D.B.; Severa, G.; Filinchuk, Y.; D’Anna, V.; Hagemann, H.; Haase, D.; Skibsted, J.; Jensen, C.M.; Jensen, T.R. Structure and Characterization of $\text{KSc}(\text{BH}_4)_4$. *J. Phys. Chem. C* **2010**, *114*, 19540–19549.
 118. Vajo, J.J.; Olson, G.L. Hydrogen Storage in Destabilized Chemical Systems. *Scripta Mater.* **2007**, *56*, 829–834.
 119. NIST Webbook. Available online: <http://webbook.nist.gov/chemistry> (accessed on 12 January 2011).
 120. Vajo, J.J.; Skeith, S.L.; Mertens, F. Reversible Storage of Hydrogen in Destabilized LiBH_4 . *J. Phys. Chem. B* **2005**, *109*, 3719–3722.

121. Aoki, M.; Miwa, K.; Noritake, T.; Kitahara, G.; Nakamori, Y.; Orimo, S.; Towata, S. Destabilization of LiBH_4 by Mixing with LiNH_2 . *Appl. Phys. A* **2005**, *80*, 1409–1412.
122. Johnson, S.R.; Anderson, P.A.; Edwards, P.P.; Gameson, I.; Prendergast, J.W.; Al-Mamouri, M.; Book, D.; Harris, I.R.; Speight, J.D.; Walton, A. Chemical Activation of MgH_2 , a New route to Superior Hydrogen Storage Materials. *Chem. Commun.* **2005**, *22*, 2823–2825.
123. Pinkerton, F.E.; Meisner, G.P.; Meyer, M.S.; Balogh, M.P.; Kundrat, M.D. Hydrogen Desorption Exceeding Ten Weight Percent from the New Quaternary Hydride $\text{Li}_3\text{BN}_2\text{H}_8$. *J. Phys. Chem. B* **2005**, *109*, 6–8.
124. Alapati, S.V.; Johnson, J.K.; Sholl, D.S. Identification of Destabilized Metal Hydrides for Hydrogen Storage Using First Principles Calculations. *J. Phys. Chem. B* **2006**, *110*, 8769–8776.
125. Cho, Y.W.; Shim, J.-H.; Lee, B.-J. Thermal Destabilization of Binary and Complex Metal Hydrides by Chemical Reaction: A Thermodynamic Analysis. *Comput. Coupling Phase Diagr. Thermochem.* **2006**, *30*, 65–59.
126. Yu, X.B.; Grant, D.M.; Walker, G.S. A New Dehydrogenation Mechanism for Reversible Multicomponent Borohydride Systems—the Role of Li-Mg Alloys. *Chem. Commun.* **2006**, *37*, 3906–3908.
127. Nakamori, Y.; Ninomiya, A.; Kitahara, G.; Aoki, M.; Noritake, T.; Miwa, K.; Kojima, Y.; Orimo, S. Dehydrating Reactions of Mixed Complex Hydrides. *J. Power Sources.* **2006**, *155*, 447–455.
128. Meisner, G.P.; Scullin, M.L.; Balogh, M.P.; Pinkerton, F.E.; Meyer, M.S. Hydrogen Release from Mixtures of Lithium Borohydride and Lithium Amide: A Phase Diagram Study. *J. Phys. Chem. B* **2006**, *110*, 4189–4192.
129. Noritake, T.; Aoki, M.; Towata, S.; Ninomiya, A.; Nakamori, Y.; Orimo, S. Crystal Structure Analysis of Novel Complex Hydrides Formed by Combination of LiBH_4 and LiNH_2 . *Appl. Phys. A* **2006**, *83*, 277–279.
130. Pinkerton, F.E.; Meyer, M.S.; Meisner, G.P.; Balogh, M.P. Improved Hydrogen Release from $\text{LiB}_{0.33}\text{N}_{0.67}\text{H}_{2.67}$ with Novel Metal Additives. *J. Phys. Chem. B* **2006**, *110*, 7967–7974.
131. Chater, P.A.; David, W.I.F.; Johnson, S.R.; Edwards, P.P.; Anderson, P.A. Synthesis and Crystal Structure of $\text{Li}_4\text{BH}_4(\text{NH}_2)_3$. *Chem. Commun.* **2006**, *23*, 2439–2441.
132. Noritake, T.; Aoki, M.; Towata, S.; Ninomiya, A.; Nakamori, Y.; Orimo, S. Crystal Structure Analysis of Novel Complex Hydrides Formed by the Combination of LiBH_4 and LiNH_2 . *Appl. Phys. A* **2006**, *83*, 277–279.
133. Alapati, S.V.; Johnson, J.K.; Sholl, D.S. Stability Analysis of Doped Materials for Reversible Hydrogen Storage in Destabilized Metal Hydrides. *Phys. Rev. B* **2007**, *76*, 104108.
134. Yang, J.; Sudik, A.; Wolverton, C. Destabilizing LiBH_4 with a Metal ($\text{M} = \text{Mg}, \text{Al}, \text{Ti}, \text{V}, \text{Cr}, \text{or Sc}$) or Metal Hydride ($\text{MH}_2 = \text{MgH}_2, \text{TiH}_2, \text{CaH}_2$). *J. Phys. Chem.* **2007**, *111*, 19134–19140.
135. Siegel, D.J.; Wolverton, C.; Ozoliņš, V. Thermodynamics Guidelines for the Prediction of Hydrogen Storage Reactions and Their Application to Destabilized Hydride Mixtures. *Phys. Rev. B* **2007**, *76*, 134102.
136. Bösenberg, U.; Doppiu, S.; Mosegaard, L.; Barkhordarian, G.; Eigen, N.; Borgschulte, A.; Jensen, T.R.; Cerenius, Y.; Gutfleisch, O.; Klassen, T.; Dornheim, M.; Bormann, R. Hydrogen Sorption Properties of MgH_2 - LiBH_4 Composites. *Acta Mater.* **2007**, *55*, 3951–3958.

137. Kang, X.-D.; Wang, P.; Ma, L.-P.; Cheng, H.-M. Reversible Hydrogen Storage in LiBH_4 Destabilized by Milling with Al. *Appl. Phys. A* **2007**, *89*, 963–966.
138. Pinkerton, F.E.; Meyer, M.S. Reversible Hydrogen Storage in the Lithium Borohydride—Calcium Hydride Coupled System. *J. Alloys Compd.* **2008**, *464*, L1–L4.
139. Wolverton, C.; Siegel, D.J.; Akbarzadeh, A.R.; Ozoliņš, V. Discovery of Novel Hydrogen Storage Materials: An Atomci Scale Computational Approach. *J. Phys.: Condens. Matter* **2008**, *20*, 064228.
140. Sudik, A.; Yang, J.; Halliday, D.; Wolverton, C. Hydrogen Storage Properties in $(\text{LiNH}_2)_2\text{-LiBH}_4\text{-(MgH}_2)_x$ Mixture ($x = 0.0\text{--}1.0$). *J. Phys. Chem. C* **2008**, *112*, 4384–4390.
141. Yang, J.; Sudik, A.; Siegel, D.J.; Halliday, D.; Drews, A.; Carter, R.O., III; Wolverton, C.; Lewis, G.J.; Sachtler, J.W.A.; Low, J.J.; Faheem, S.A.; Lesch, D.A.; Ozoliņš, V. A Self-Catalyzing Hydrogen-Storage Material. *Angew. Chem. Int. Ed.* **2008**, *47*, 882–887.
142. Alapati, S.V.; Johnson, J.K.; Sholl, D.S. Large-Scale Screening of Metal Hydride Mixtures for High-Capacity Hydrogen Storage from First-Principle Calculations. *J. Phys. Chem. C* **2008**, *112*, 5258–5262.
143. Purewal, J.; Hwang, S.-J.; Bowman, R.C., Jr.; Rönnebro, E.; Fultz, B.; Ahn, C. Hydrogen Sorption Behavior of the $\text{ScH}_2\text{-LiBH}_4$ System: Experimental Assesment of Chemical Destabilization Effects. *J. Phys. Chem. C* **2008**, *112*, 8481–8485.
144. Jin, S.-A.; Lee, Y.-S.; Shim, J.-H.; Cho, Y.W. Reversible Hydrogen Storage in $\text{LiBH}_4\text{-MgH}_2$ ($M = \text{Ce, Ca}$). *J. Phys. Chem. C* **2008**, *112*, 9520–9524.
145. Wan, X.; Markmaitree, T.; Osborn, W.; Shaw, L.L. Nanoengineering-Enabled Solid-State Hydrogen Uptake and Release in the LiBH_4 Plus MgH_2 System. *J. Phys. Chem. C* **2008**, *112*, 18232–18243.
146. Langmi, H.W.; McGrady, G.S. Ternary Nitrides for Hydrogen Storage: Li-B-N, Li-Al-N and Li-Ga-N Systems. *J. Alloys Compd.* **2008**, *466*, 287–292.
147. Jin, S.-A.; Shim, J.-H.; Cho, Y.W.; Yi, K.-W.; Zabara, O.; Fichtner, M. Reversible Hydrogen Storage in $\text{LiBH}_4\text{-Al-LiH}$ Composite Powder. *Scripta Mater.* **2008**, *58*, 963–965.
148. Fan, M.-Q.; Sun, L.-X.; Zhang, Y.; Xu, F.; Zhang, J.; Chu, H.-L. The Catalytic Effect of Additive Nb_2O_5 on the Reversible Hydrogen Storage Performances of $\text{LiBH}_4\text{-MgH}_2$ Composite. *Int. J. Hydrogen Energy.* **2008**, *33*, 74–80.
149. Tang, W.S.; Wu, G.T.; Liu, T.; Wee, A.T.S.; Yong, C.K.; Xiong, Z.; Hor, T.S.; Chen, P. Cobalt-Catalyzed Hydrogen Desorption from the $\text{LiNH}_2\text{-LiBH}_4$ System. *Dalton Trans.* **2008**, *18*, 2395–2399.
150. Bösenberg, U.; Vainio, U.; Pranzas, P.K.; Bellosta von Colbe, J.M.; Goerigk, G.; Welter, E.; Dornheim, M.; Schreyer, A.; Bormann, R. On the Chemical State and Distribution of Zr- and V-Based Additives in Reactive Hydride Composites. *Nanotechnology* **2009**, *20*, 204003.
151. Wang, P.J.; Ma, L.P.; Fang, Z.Z.; Kang, X.D.; Wang, P. Improved Hydrogen Storage Properties of Li-Mg-B-H System by Milling with Titanium Trifluoride. *Energy Environ. Sci.* **2009**, *2*, 120–123.
152. Du, A.J.; Smith, S.C.; Yao, X.D.; Sun, C.H.; Li, L. Lu, G.Q. First Principle Study of Hydrogen of MgB_2 : An Important Step toward Reversible Hydrogen Storage in the Coupled $\text{LiBH}_4/\text{MgH}_2$ System. *J. Nanosci. Nanotechnol.* **2009**, *9*, 4388–4391.

153. Yang, J.; Hirano, S. Improving the Hydrogen Reaction Kinetics of Complex Hydrides. *Adv. Mater.* **2009**, *21*, 1–6.
154. Graetz, J.; Chaudhuri, S.; Salguero, T.T.; Vajo, J.J.; Meyer, M.S.; Pinkerton, F.E. Local bonding and atomic environments in Ni-catalyzed complex hydrides. *Nanotechnology* **2009**, *20*, 204007.
155. Sudik, A.; Yang, J.; Siegel, D.J.; Wolverton, C.; Carter, R.O., III; Drews, A.R. Impact of Stoichiometry on the Hydrogen Storage Properties of $\text{LiNH}_2\text{-LiBH}_4\text{-MgH}_2$ Ternary Composites. *J. Phys. Chem. C* **2009**, *113*, 2004–2013.
156. Walker, G.S.; Grant, D.M.; Price, T.C.; Yu, X.B.; Legrand, V. High Capacity Multicomponent Hydrogen Storage Materials: Investigation of the Effect of Stoichiometry and Decomposition Conditions on the Cycling Behaviour of $\text{LiBH}_4\text{-MgH}_2$. *J. Power Sources* **2009**, *194*, 1128–1134.
157. Mao, J.F.; Guo, Z.P.; Liu, H.K.; Yu, X.B. Reversible Hydrogen Storage in Titanium-Catalyzed $\text{LiAlH}_4\text{-LiBH}_4$. *J. Alloys. Compd.* **2009**, *487*, 434–438.
158. Puzkiel, J.A.; Gennari, F.C. Reversible Hydrogen Storage in Metal-Doped Mg-LiBH_4 Composites. *Scripta Mater.* **2009**, *60*, 667–670.
159. Zhang, Y.; Tian, Q.; Chu, H.L.; Zhang, J.; Sun, L.; Sun, J.; Wen, Z. Hydrogen De/Resorption Properties of the $\text{LiBH}_4\text{-MgH}_2\text{-Al}$ System. *J. Phys. Chem. C* **2009**, *113*, 21964–21969.
160. Wu, H.; Zhou, M.I.; Wang, K.; Udovic, T.J.; Rush, J.J.; Yildirim, T.; Bendersky, L.A.; Gross, A.F.; van Atta, S.L.; Vajo, J.J.; Pinkerton, F.E.; Meyer, M.S. Size Effects on the Hydrogen Storage Properties of Nanoscaffolded $\text{Li}_3\text{BN}_2\text{H}_8$. *Nanotechnology* **2009**, *20*, 204002.
161. Pinkerton, F.E.; Meyer, M.S. Hydrogen Desorption Behavior of Nickel-Chloride-Catalyzed Stoichiometric $\text{Li}_4\text{BN}_3\text{H}_{10}$. *J. Phys. Chem. C* **2009**, *113*, 11172–11176.
162. Kim, J.W.; Friedrichs, O.; Ahn, J.-P.; Kim, D.H.; Kim, S.C.; Remhof, A.; Chung, H.-S.; Lee, J.; Shim, J.-H.; Cho, Y.W.; Züttel, A.; Oh, K.H. Microstructural Change of $2\text{LiBH}_4/\text{Al}$ with Hydrogen Sorption cycling: Separation of Al and B. *Scripta Mater.* **2009**, *60*, 1089–1092.
163. Friedrichs, O.; Kim, J.W.; Remhof, A.; Buchter, F.; Borgschulte, A.; Wallacher, D.; Cho, Y.W.; Fichtner, M.; Oh, K.H.; Züttel, A. The Effect of Al on the Hydrogen Sorption Mechanism of LiBH_4 . *Phys. Chem. Chem. Phys.* **2009**, *11*, 1515–1520.
164. Blanchard, D.; Shi, Q.; Boothroyd, C.B.; Vegge, T. Reversibility of Al/Ti Modified LiBH_4 . *J. Phys. Chem. C* **2009**, *113*, 14059–14066.
165. Zhang, Y.; Tian, Q.; Zhang, J.; Liu, S.-S.; Sun, L.-X. The Dehydrogenation Reactions and Kinetics of $2\text{LiBH}_4\text{-Al}$ Composite. *J. Phys. Chem. C* **2009**, *113*, 18424–18430.
166. Singer, J.P.; Meyer, M.S.; Speer, R.M., Jr.; Fischer, J.E.; Pinkerton, F.E. Determination of the Phase Behavior of $(\text{LiNH}_2)_c(\text{LiBH}_4)_{1-c}$ Quaternary Hydride through in Situ X-ray Diffraction. *J. Phys. Chem. C* **2009**, *113*, 18927–18934.
167. Li, W.; Vajo, J.J.; Cumberland, R.W.; Liu, P.; Hwang, S.-J.; Kim, C.; Bowman, R.C., Jr. Hydrogenation of Magnesium Nickel Boride for Reversible Hydrogen Storage. *Phys. Chem. Lett.* **2010**, *1*, 69–72.
168. Wang, P.-J.; Fang, Z.-Z.; Ma, L.-P.; Kang, X.-D.; Wang, P. Effect of Carbon Addition on Hydrogen Storage Behaviors of Li-Mg-B-H System. *Int. J. Hydrogen Energy* **2010**, *35*, 3072–3075.

169. Shim, J.-H.; Lim, J.-H.; Rather, S.-U.; Lee, Y.-S.; Reed, D.; Kim, Y.; Book, D.; Cho, Y.W. Effect of Hydrogen Back Pressure on Dehydrogenation Behavior of LiBH₄-Based Reactive Hydride Composites. *Phys. Chem. Lett.* **2010**, *1*, 59–63.
170. Deprez, E.; Muñoz-Márquez, M.A.; Roldán, M.A.; Prestipino, C.; Javier Palomares, F.; Bonatto Minella, C.; Bösenberg, U.; Dornheim, M.; Bormann, R.; Fernández, A.; Oxidation State and Local Structure of Ti-Based Additives in the Reactive Hydride Composite 2 LiBH₄ + MgH₂. *J. Phys. Chem.* **2010**, *114*, 3309–3317.
171. Bösenberg, U.; Kim, J.W.; Gossler, D.; Eigen, N.; Jensen, T.G.; Bellosta von Colbe, J.M.; Zhou, Y.; Dahms, M.; Kim, D.H.; Günther, R.; Cho, Y.W.; Oh, K.H.; Klassen, T.; Bormann, R.; Dornheim, M. Role of Additives in LiBH₄-MgH₂ Reactive Hydride Composites for Sorption Kinetics. *Acta Mater.* **2010**, *58*, 3381–3389.
172. Price, T.C.; Grant, D.M.; Legrand, V.; Walker, G.S. Enhanced Kinetics for the LiBH₄:MgH₂ Multi-Component Hydrogen Storage System—The Effects of Stoichiometry and Decomposition Environment on Cycling Behaviour. *Int. J. Hydrogen Energy* **2010**, *35*, 4154–4161.
173. Somer, M.; Acar, S.; Koz, C.; Kokal, I.; Höhn, P.; Cardoso-Gil, R.; Aydemir, U.; Akselrud, L. α - and β -Na₂[BH₄][NH₂]: Two Modifications of a Complex Hydride in the System NaNH₂-NaBH₄; Syntheses, Crystal Structures, Thermal Analyses, Mass and Vibrational Spectra. *J. Alloys Compd.* **2010**, *491*, 98–105.
174. Yu, X.B.; Guo, Y.H.; Sun, D.L.; Yang, Z.X.; Ranjbar, A.; Guo, Z.P.; Liu, H.K.; Dou, S.X. A Combined Hydrogen Storage System of Mg(BH₄)₂-LiNH₂ with Favorable Dehydrogenation. *J. Phys. Chem. C* **2010**, *114*, 4733–4737.
175. Mao, J.; Guo, Z.; Leng, H.; Wu, Z.; Guo, Y.; Yu, X.; Liu, H. Reversible Hydrogen Storage in Destabilized LiAlH₄-MgH₂-LiBH₄ Ternary-Hydride System Doped with TiF₃. *J. Phys. Chem. C* **2010**, *114*, 11643–11649.
176. Ravnsbæk, D.B.; Jensen, T.R. Tuning hydrogen storage properties and reactivity: Investigation of the LiBH₄-NaAlH₄ system. *J. Phys. Chem. Sol.* **2010**, *71*, 1144–1149.
177. Mauron, P.; Biemann, M.; Remhof, A.; Züttel, A.; Shim, J.-K.; Cho, Y.W. Stability of the LiBH₄/CeH₂ Composite System Determined by Dynamic pcT Measurements. *J. Phys. Chem. C* **2010**, *114*, 16801–16805.
178. Bösenberg, U.; Ravnsbæk, D.B.; Hagemann, H.; D’Anna, V.; Minella, C.B.; Pistidda, C.; van Beek, W.; Jensen, T.R.; Bormann, R.; Dornheim, M. Pressure and Temperature Influence on the Desorption Pathway of the LiBH₄-MgH₂ Composite System. *J. Phys. Chem. C* **2010**, *114*, 15212–15217.
179. Zeng, L.; Miyaoka, H.; Ichikawa, T.; Kojima, Y. Superior Hydrogen Exchange Effect in the MgH₂-LiBH₄ System. *J. Phys. Chem. C* **2010**, *114*, 13132–13135.
180. Crosby, K.; Shaw, L.L. Dehydriding and re-hydriding properties of high-energy ball milled LiBH₄ + MgH₂ mixture. *Int. J. Hydrogen Energy* **2010**, *35*, 7519–7529.
181. Choudhury, P.; Bhethanabotla, V.R.; Stefanakos, E. First principles study to identify the reversible reaction step of a multinary hydrogen storage “Li-Mg-B-N-H” system. *Int. J. Hydrogen Energy* **2010**, *35*, 9002–9011.
182. Shaw, L.L.; Wan, X.; Hu, J.Z.; Kwak, J.H.; Yang, Z. Solid-State Hydriding Mechanism in the LiBH₄-MgH₂ System. *J. Phys. Chem. C* **2010**, *114*, 8089–8098.

183. Garroni, S.; Milanese, C.; Girella, A.; Marini, A.; Mulas, G.; Menéndez, E.; Pistidda, C.; Dornheim, M.; Suriñach, S.; Baró, M.D. Sorption Properties of NaBH₄/MH₂ (M = Mg, Ti) Powder System. *Int. J. Hydrogen Energy* **2010**, *35*, 5434–5441.
184. Gennari, F.C.; Puzskiel, J.A. Enhanced Hydrogen Sorption Kinetics of Mg₅₀Ni-LiBH₄. *J. Power Sources* **2010**, *195*, 3266–3274.
185. Hattrick-Simpers, J.R.; Maslar, J.E.; Niemann, M.U.; Chium, C.; Srinivasan, S.S.; Stefanakos, E.K.; Bendersky, L.A. Raman Spectroscopic Observation of Dehydrogenation in Ball-Milled LiNH₂-LiBH₄-MgH₂ Nanoparticles. *Int. J. Hydrogen Energy* **2010**, *35*, 6323–6331.
186. Barkhordarian, G.; Klassen, T.; Dornheim, M.; Bormann, R. Unexpected Kinetic Effect of MgB₂ in Reactive Composites Containing Complex borohydrides. *J. Alloys Compd.* **2007**, *440*, L18–L21.
187. Barkhordarian, G.; Jensen, T.R.; Doppiu, S.; Bolsenberg, U.; Borgschulte, A.; Gremaud, R.; Cerenius, Y.; Dornheim, M.; Klassen, T.; Bormann, R. Formation of Ca(BH₄)₂ from Hydrogenation of CaH₂ + MgB₂ Composite. *J. Phys. Chem. C* **2008**, *112*, 2743–2749.
188. Hu, J.Z.; Kwak, J.H.; Y, Z.; Wan, X.; Shaw, L.L. Direct Observation of Ion Exchange in Mechanically Activated LiH + MgB₂ System Using Ultrahigh Field Nuclear Magnetic Resonance Spectroscopy. *Appl. Phys. Lett.* **2009**, *94*, 141905.
189. Gosalawit-Utke, R.; Bellosta von Colbe, J.M.; Dornheim, M.; Jensen, T.R.; Cerenius, Y.; Minella, C.B.; Peschke, M.; Bormann, R. LiF-MgB₂ System for Reversible Hydrogen Storage. *J. Phys. Chem. C* **2010**, *114*, 10291–10296.
190. Gonzalez-Silveira, M.; Gremaud, R.; Schreuders, H.; van Setten M.J.; Batyrev, E.; Rougier, A.; Dupont, L.; Bardají, E.G.; Lohstroh, W.; Dam, B. In-Situ Deposition of Alkali and Alkaline Earth Hydride Thin Films To Investigate the Formation of Reactive Hydride Composites. *J. Phys. Chem. C* **2010**, *114*, 13895–13901.
191. Rongeat, C.; D’Anna, V.; Hagemann, H.; Borgschulte, A.; Züttel, A.; Schultz, L.; Gutfleisch, O. Effect of Additives on the Synthesis and Reversibility of Ca(BH₄)₂. *J. Alloys Compd.* **2010**, *493*, 281–287.
192. Kim, Y.; Reed, D.; Lee, Y.-S.; Shim, J.-H.; Han, H.N.; Book, D.; Cho, Y.W. Hydrogenation Reaction of CaH₂-CaB₆-Mg Mixture. *J. Alloys Compd.* **2010**, *492*, 597–600.
193. Bogdanović, B.; Schwickardi, M. Ti-doped alkali metal aluminium hydrides as potential novel reversible hydrogen storage materials. *J. Alloy. Compd.* **1997**, *253–254*, 1–9.
194. Au, M.; Jurgensen, A. Modified Lithium Borohydrides for Reversible Hydrogen Storage. *J. Phys. Chem. B* **2006**, *110*, 7062–7067.
195. Au, M.; Jurgensen, A.; Zeigler, K. Modified Lithium Borohydrides for Reversible Hydrogen Storage (2). *J. Phys. Chem. B* **2006**, *110*, 26482–26487.
196. Yu, X.B.; Wu, Z.; Chen, Q.R.; Li, Z.L.; Weng, B.C.; Huang, T.S. Improved Hydrogen Storage Properties of LiBH₄ Destabilized by Carbon. *Appl. Phys. Lett.* **2007**, *90*, 034106.
197. Zhang, Y.; Zhang, W.-S.; Wang, A.-Q.; Sun, L.-X.; Fan, M.-Q.; Chu, H.-L. Sun, J.-C.; Zhang, T. LiBH₄ Nanoparticles Supported by Disordered Mesoporous Carbon: Hydrogen Storage Performances and Destabilization Mechanisms. *Int. J. Hydrogen Energy* **2007**, *32*, 3976–3980.

198. Varin, R.A.; Chiu, C.; Wronski, Z.S.; Calka, A. The Effects of Oxidized and Oxide-Free Boron on the Mg-B-H Nanohydrides Transformation in the Nearly Nanosized Powders. *Solid State Phenom.* **2007**, *128*, 47–52.
199. Mosegaard, L.; Møller, B.; Jørgensen, J.-E.; Filinchuk, Y.; Cerenius, Y.; Hanson, J.; Dimasi, E.; Besenbacher, F.; Jensen, T.R. Reactivity of LiBH₄: In Situ Synchrotron Radian Powder X-ray Diffraction Study. *J. Phys. Chem. C* **2008**, *112*, 1299–1303.
200. Yin, L.; Wang, P.; Fang, Z.Z.; Cheng, H. Thermodynamically Tuning LiBH₄ by Fluorine Anion Doping for Hydrogen Storage: A Density functional Study. *Chem. Phys. Lett.* **2008**, *450*, 318–321.
201. Zhang, Y.; Zhang, W.-S.; Fan, M.-Q.; Liu, S.-S.; Chu, H.-L.; Zhang, Y.-H.; Gao, X.-Y.; Sun, L.-X. Enhanced Hydrogen Storage Performance of LiBH₄-SiO₂-TiF₃ Composite. *J. Phys. Chem. C* **2008**, *112*, 4005–4110.
202. Fang, Z.Z.; Kang, X.D.; Dai, H.B.; Zhang, M.J.; Wang, P.; Cheng, H.M. Reversible Dehydrogenation of LiBH₄ Catalyzed by As-Prepared Sing-Walled Carbon Nanotubes. *Scripta Mater.* **2008**, *58*, 922–925.
203. Xu, J.; Yu, X.B.; Zou, Z.Q.; Li, Z.L.; Wu, Z.; Akins, L.D.; Yang, H. Enhanced Dehydrogenation of LiBH₄ Catalyzed by Carbon-Supported Pt Nanoparticles. *Chem. Commun.* **2008**, *44*, 5740–5742.
204. Fang, Z.-Z.; Kang, X.-D.; Wang, P.; Cheng, H.-M. Improved Reversible Dehydrogenation of Lithium Borohydride by Milling with As-Prepared Single-Walled Carbon Nanotubes. *J. Phys. Chem. C* **2008**, *112*, 17023–17029.
205. Au, M.; Jurgensen, A.R.; Spencer, W.A.; Anto, D.A.; Pinkerton, F.E.; Hwang, S.-J.; Kim, C.; Bowman, R.C., Jr. Stability and Reversibility of Lithium Borohydrides Doped by Metal Halides and Hydrides. *J. Phys. Chem. C* **2008**, *112*, 18661–18671.
206. Yu, X.B.; Grant, D.M.; Walker, G.S. Dehydrogenation of LiBH₄ Destabilized with Various Oxides. *J. Phys. Chem. C* **2009**, *113*, 17945–17949.
207. Arnbjerg, L.M.; Ravnsbæk, D.B.; Filinchuk, Y.; Vang, R.T.; Cerenius, Y.; Besenbacher, F.; Jørgensen, J.-E.; Jakobsen, H.J.; Jensen, T.R. Structure and Dynamics for LiBH₄-LiCl Solid Solutions. *Chem. Mater.* **2009**, *21*, 5772–5782.
208. Guo, Y.H.; Yu, X.B.; Gao, L.; Xia, G.L.; Guo, Z.P.; Liu, H.K. Significantly Improved Dehydrogenation of LiBH₄ Destabilized by TiF₃. *Energy Environ. Sci.* **2010**, *3*, 465–470.
209. Fang, Z.Z.; Kang, X.D.; Wang, P. Improved Hydrogen Storage Properties of LiBH₄ by Mechanical Milling with Various Carbon Additives. *J. Int. Hydrogen Energy* **2010**, *35*, 8247–8252.
210. Zhang, B.J.; Liu, B.H. Hydrogen Desorption from LiBH₄ destabilized by chlorides of transition metal Fe, Co, and Ni. *Int. J. Hydrogen Energy* **2010**, *35*, 7288–7294.
211. Gutowska, A.; Li, L.; Shin, Y.; Wang, C.M.; Li, X.S.; Linehan, J.C.; Smith, R.S.; Kay, B.D.; Schmid, B.; Shaw, W.; Gutowski, M.; Autrey, T. Nanoscaffold Mediates Hydrogen Release and the Reactivity of Ammonia Borane. *Angew. Chem. Int. Ed.* **2005**, *44*, 3578.
212. Gross, A.F.; Vajo, J.J.; van Atta, S. L.; Olson, G.L. Enhanced Hydrogen Storage Kinetics of LiBH₄ in Nanoporous Carbon Scaffolds. *J. Phys. Chem. C* **2008**, *112*, 5651–5657.

213. Fang, Z.Z.; Wang, P.; Rufford, T.E.; Kang, X.D.; Lu, G.Q.; Cheng, H.M. Kinetic- and Thermodynamic-Based Improvements of Lithium Borohydride Incorporated Into Activated Carbon. *Acta Mater.* **2008**, *56*, 6257–6263.
214. Cahen, S.; Eymery, J.-B.; Janot, R.; Tarascon, J.-M. Improvement of the LiBH₄ Hydrogen Desorption by Inclusion into Mesoporous Carbons. *J. Power Sources* **2009**, *189*, 902–908.
215. Ingleson, M.J.; Barrio, J.P.; Bacsá, J.; Steiner, A.; Darling, G.R.; Jones, J.T.A.; Khimyak, Y.Z.; Rosseinsky, M.J. Magnesium Borohydride Confined in a Metal–Organic Framework: A Preorganized System for Facile Arene Hydroboration. *Angew. Chem. Int. Ed.* **2009**, *48*, 2012–2016.
216. Fichtner, M.; Zhao-Karger, Z.; Hu, J.; Roth, A.; Weidler, P. The Kinetic Properties of Mg(BH₄)₂ Infiltrated in Activated Carbon. *Nanotechnology* **2009**, *20*, 204029.
217. Ngene, P.; Adelhelm, P.; Beale, A.M.; de Jong, K.P.; de Jongh, P.E. LiBH₄/SBA-15 Nanocomposites Prepared by Melt infiltration under Hydrogen pressure: Synthesis and Hydrogen Sorption Properties. *J. Phys. Chem. C* **2010**, *114*, 6163–6168.
218. Shane, D.T.; Corey, R.L.; McIntosh, C.; Rayhel, L.H.; Bowman, R.C., Jr.; Vajo, J.J.; Gross, A.F.; Conradi, M.S. LiBH₄ in Carbon Aerogel Nanoscaffolds: An NMR Study of Atomic Motions. *J. Phys. Chem. C* **2010**, *114*, 4008–4014.
219. Liu, X.; Peaslee, D.; Jost, C.Z.; Majzoub, E.H. Controlling the Decomposition Pathway of LiBH₄ via Confinement in Highly Ordered Nanoporous Carbon. *J. Phys. Chem. C* **2010**, *114*, 14036–14041.
220. Ngene, P.; van Zwienen, M.R.; de Jongh, P.E. Reversibility of the hydrogen desorption from LiBH₄: A synergetic effect of nanoconfinement and Ni addition. *Chem. Comm.* **2010**, *46*, 8201–5203.
221. Nielsen, T.K.; Bösenber, U.; Gosalawit, R.; Dornheim, M.; Cerenius, Y.; Besenbacher, F.; Jensen, T.R. A Reversible Nanoconfined Chemical Reaction. *ACS NANO* **2010**, *4*, 3903–3908.
222. Sartori, S.; Knudsen, K.D.; Zhao-karger, Z.; Bardaji, E.G.; Muller, J.; Fichtner, M.; Hauback, B.C. Sartori, S.; Knudsen, K.D.; Zhao-karger, Z.; Bardaji, E.G.; Muller, J.; Fichtner, M.; Hauback, B.C. Nanoconfined Magnesium Borohydride for Hydrogen Storage Application Investigation by SANS and SAXS. *J. Phys. Chem. C* **2010**, *114*, 18785–18789.